
Gulf of Mexico Gas Hydrate Joint Industry Project Leg II: Green Canyon 955 Site Summary

Dan McConnell¹, Ray Boswell², Timothy Collett³, Matthew Frye⁴, William Shedd⁵, Gilles Guerin⁶, Ann Cook⁶, Stefan Mrozewski⁶, Rebecca Dufrene⁵, & Paul Godfriaux⁵

Abstract

In April and May of 2009 the Gulf of Mexico Gas Hydrate Joint Industry Project conducted its second field program (Leg II) with the semi-submersible Helix *Q-4000* drillship. The three-week expedition drilled seven logging-while-drilling (LWD) holes at three sites that tested a variety of geologic/geophysical models for the occurrence of gas hydrate in sand reservoirs in the deepwater Gulf of Mexico. At the GC 955 site, high saturation gas hydrate deposits in sands were found, where predicted, at two of the three holes. The full research-level LWD assembly deployed for Leg II collected data on formation lithology and porosity, and included quadrapole acoustic and high-resolution 3-D resistivity logs. No samples, only LWD data, were collected in Leg II. The three holes in GC 955 were drilled where a wide and thick late-Pleistocene channel complex had been raised and fractured by salt uplift. A four-way closure with numerous amplitude anomalies consistent with the inferred base of gas hydrate stability is near-to but west of the channel axis. The first well (GC 955-I) was drilled very close to the channel axis in a location with muted geophysical indications of gas hydrate. More than 300 ft of porous sands were encountered as predicted; however the sands contained primarily water – with only modest indications of gas hydrate. The next hole (GC 955-H) targeted sands higher in the four-way closure. Fracture filling gas hydrate was detected above the deeper sand target, and, at the target. At the primary target, 98 ft of sand fully saturated with gas hydrate with little to no gas beneath. A third well (GC 955-Q) also encountered at least 35 ft of fully saturated

gas hydrate-bearing sand at the target depth, but drilling was aborted because of a gas hydrate dissociation event or penetration of free gas and subsequent gas flow. The JIP's discovery of thick gas hydrate-bearing sands at the GC 955 site validates the integrated geological and geophysical approach used in the pre-drill site selection and provides increased confidence in prior assessments of gas hydrate volumes in the Gulf of Mexico.

Introduction

In April 2009, the Gulf of Mexico Gas Hydrate Joint Industry Program (JIP) conducted its Leg II operations at Sites in Alaminos Canyon block 21 (AC 21), Walker Ridge block 313 (WR 313), and Green Canyon block 955 (GC 955) in the northern Gulf of Mexico (Figure [F1](#)). The primary objectives of the JIP Leg II drilling program was to determine the occurrence of gas hydrate within sand reservoirs in the Gulf of Mexico, to assess current approaches for interpreting gas hydrate occurrence from geologic and geophysical data, and to determine the most suitable sites for additional drilling and coring in future phases of the JIP program. Initial summaries of JIP Leg II operations, scientific results, and logging-while-drilling data collection methods are provided by Collett *et al.* (2009), Boswell *et al.* (2009), and Mrozewski *et al.* (2009) respectively. This report describes the scientific rationale and initial results for the LWD program conducted at the GC 955 Site. Hutchinson *et al.* (2009) provides a review of the analyses conducted to select the targets to be permitted for possible drilling. A detailed review of logging-while-drilling (LWD) operations

¹AOA Geophysics Inc.
2500 Tanglewilde Street
Houston, TX 77063
E-mail:
dan_mcconnell@aoageophysics.com

²National Energy Technology Laboratory
U.S. Department of Energy
P.O. Box 880
Morgantown, WV 26507
E-mail:
ray.boswell@netl.doe.gov

³US Geological Survey
Denver Federal Center, MS-939
Box 25046
Denver, CO 80225
E-mail:
tcollett@usgs.gov

⁴Minerals Management Service
381 Elden St.
Herndon, VA 20170
E-mail:
matt.frye@mms.gov

⁵Minerals Management Service
1201 Elmwood Park Blvd.
New Orleans, LA 70123-2394
E-mail:
Dufrene: rebecca.dufrene@mms.gov
Godfriaux: paul.godfriaux@mms.gov
Shedd: william.shedd@mms.gov

⁶Borehole Research Group
Lamont-Doherty Earth Observatory
of Columbia University
Palisades, NY 10964
E-mail:
Cook: acook@ldeo.columbia.edu
Guerin: guerin@ldeo.columbia.edu
Mrozewski: stefan@ldeo.columbia.edu

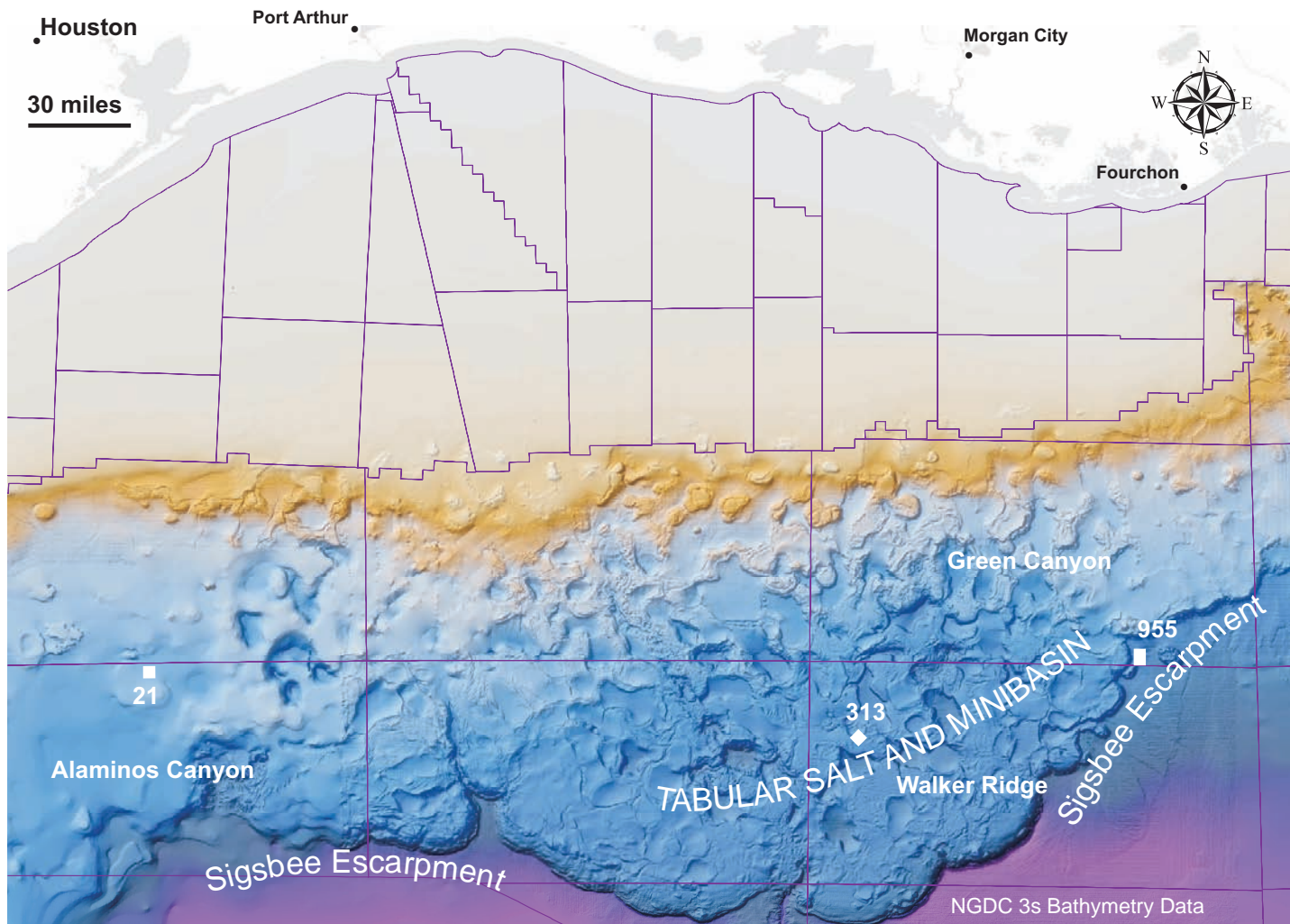


Figure F1: Northwestern Gulf of Mexico showing tabular salt and mini-basin province, Sigsbee Escarpment and AC 21, WR 313, and GC 955 sites.

and acquired data from the GC 955 site is provided by Guerin *et al.* (2009).

The JIPs selection of sites for drilling in Leg II was based on an analysis of the various elements needed to support a gas hydrate petroleum system (appropriate temperatures and pressures, gas and water sources and migration pathways) with the likely presence of sand reservoirs (needed to enable gas hydrate concentrations to high levels). In addition, the site selection process also incorporated attempts to directly detect and quantify gas hydrates from seismic data (Hutchinson *et al.*, 2009). All of these elements were seen in the GC 955 area, providing a multitude of potential, high value sites for the JIP program.

The prospectivity of the GC 955 site was based initially on the work of McConnell (2000) and Heggland (2004). Although neither author mentioned the potential for gas

hydrate deposits in the area, both described geophysical indications for ample gas sourcing, clear gas migration pathways into the shallow sediments afforded by extensive faulting, and presence of thick sand reservoirs associated with a large and persistent Pleistocene channel-levee complex. In addition, data from seismic in conjunction with log data from an existing industry well (the GC 955 #001) indicated that a thick, sand-prone section likely spans the base of gas hydrate stability (Figure F2). As a result, the GC 955 site was proposed to the JIP site selection effort by the AOA Geophysics team in early 2006. Subsequent analyses conducted by the AOA Geophysics team to determine the potential depth of the gas hydrate stability field from pressure, temperature and gas composition data (Figure F3) indicated that the observed distribution of anomalous high-amplitude reflectors are consistent with the inferred base of gas hydrate stability (BGHS). To estimate whether the target reservoir was within the gas hydrate stability

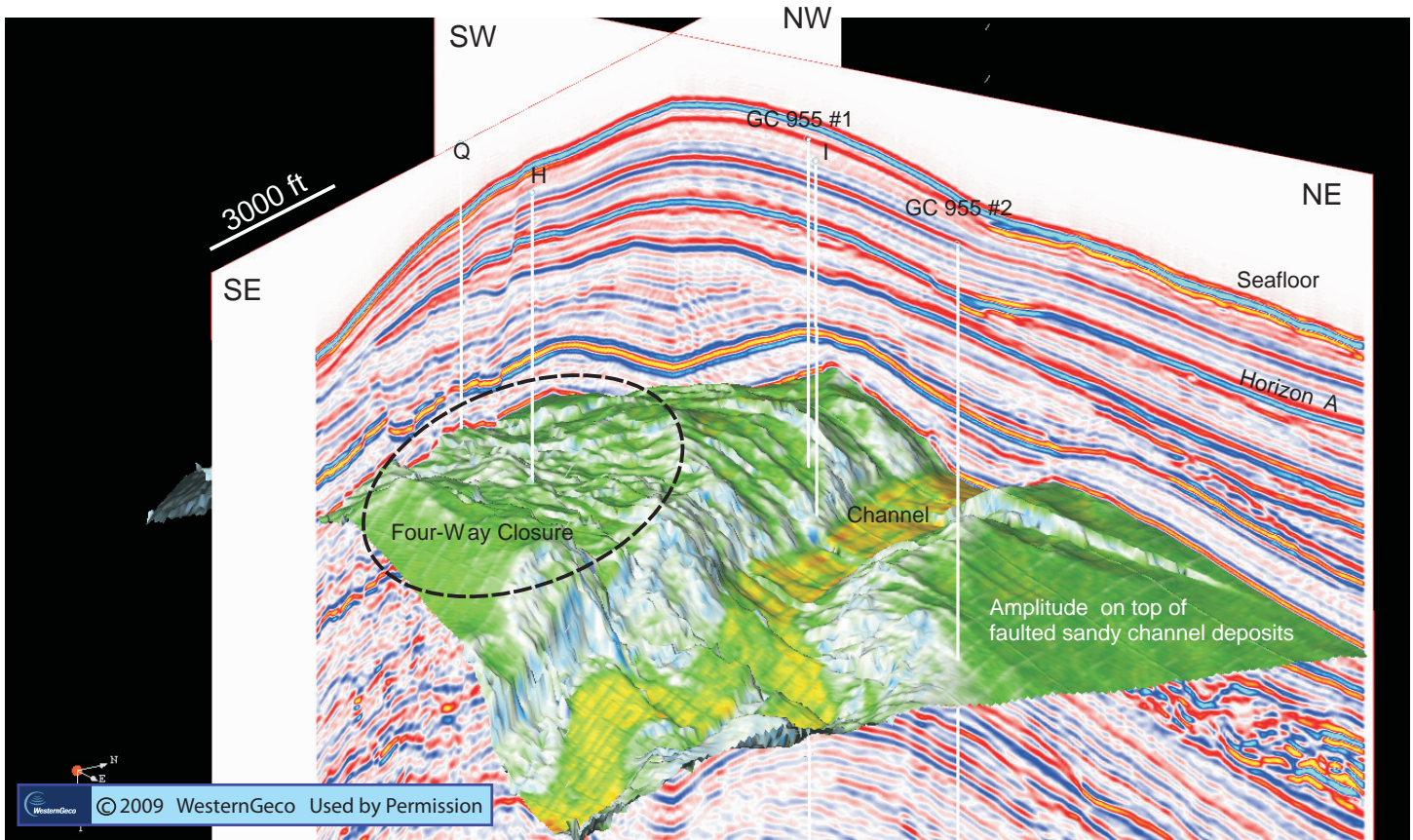


Figure F2: Perspective view from 3-D seismic of top of channel facies showing JIP and industry well penetrations, and four-way closure. Background seismic data courtesy of WesternGeco.

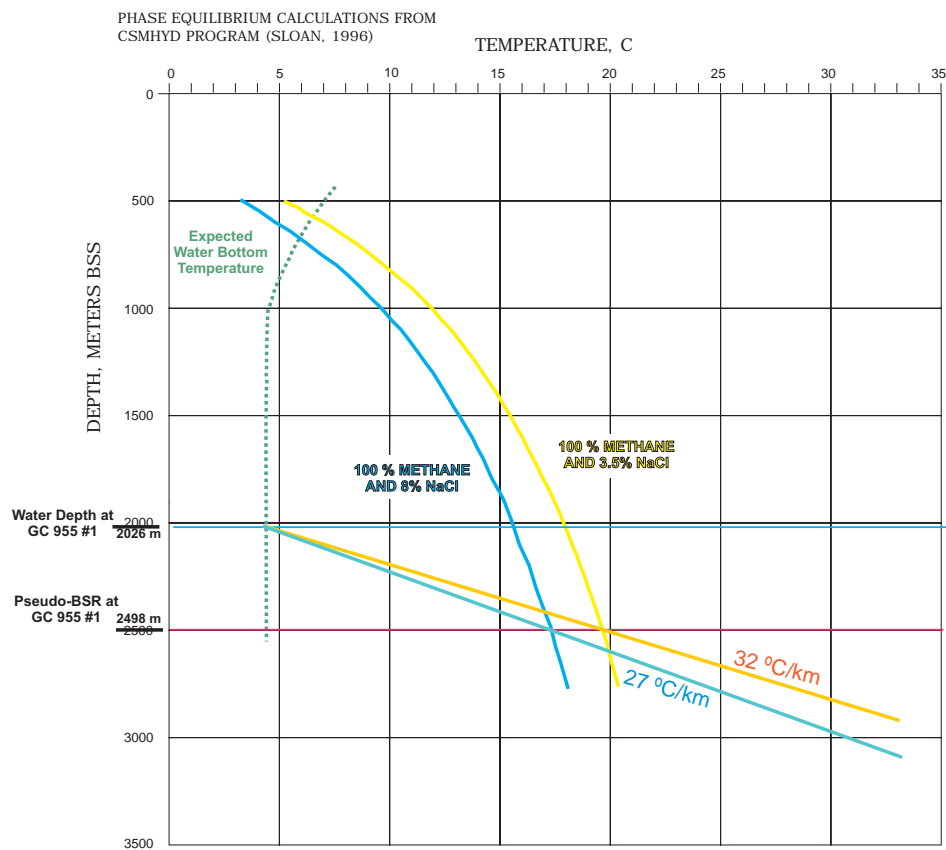


Figure F3: Gas hydrate phase stability diagram for GC 955.

zone, temperature, salinity, and pressure conditions were modeled by assuming a seafloor temperature of 4 °C, normal seawater in the pore space, and that the trend of shallowest gas at GC 955 #1 represented the base of gas hydrate stability at hydrostatic pressure. The resulting geothermal gradient of 32 °C/km is considered to be a reasonable value for sediments above shallow salt in the Gulf of Mexico (Nagihara and Smith, 2008). The geothermal gradient and pressure estimates place the target reservoir facies depths within or near the BGHS.

In 2008, seismic data under license to Chevron were forwarded to AOA Geophysics to develop potential gas hydrate targets for JIP Leg II. Numerous prospective targets were identified that tested a variety of geologic settings within the block. Targets were developed within and proximal to the most prominent channel features, as well as within a salt-cored, domal structure in the southwestern corner of the block. This structure features the most prospective geophysical anomalies and the strongest indicators of gas occurrence. The highly-faulted structure displays little lateral continuity of the reflections (Figure F4) and a complex array of responses that suggested the close association of both free gas (strong leading troughs) and gas hydrate (strong leading peaks). Despite numerous clear migration pathways further up in the section, afforded not only by faults but by the inferred presence of permeable reservoirs, these amplitudes were not present in the shallower section, suggesting that gas hydrate may be serving as a seal, restricting the vertical movement of gas.

Targets identified in the Chevron licensed 3-D seismic amplitude data were then further refined using data over GC 955 and one km south in GC 999 provided by JIP member Western Geco. Impedance and gas hydrate saturation models were produced from the Western Geco 3-D volumes using techniques as described in Dai *et al.* (2009). Other seismic-derived 3-D volumes produced in the gas hydrate modeling process include interval velocity, Poisson's ratio, V_p/V_s , compressional impedance, shear impedance, and gas hydrate saturations derived from both compressional impedance and the shear impedance seismic volumes. In addition to providing an opportunity to test the direct indicators of gas hydrate as determined through the seismic analyses, GC 955 provided opportunities to test for the occurrence of gas hydrate that may not be well imaged in seismic data, including highly heterogeneous, tabular, and steeply inclined occurrences related to fault zones,

or gas hydrate of low or transitional concentrations that resulted in lack of strong seismic reflectors.

GC 955 Gas Hydrate Petroleum System

The nine-square mile GC 955 lease block is approximately five miles basinward from Green Canyon proper, a reentrant along the Sigsbee Escarpment, approximately 146 miles south of Fourchon, Louisiana (Figure F5). The Sigsbee Escarpment is the seafloor expression of a large Jurassic allochthonous salt nappe that mobilized and extruded into and carries shallower sediments basinward by gravitational processes (Amery, 1969; Rowan, 1999). The Sigsbee Escarpment, in general, represents the seaward limit of salt extrusion, but two salt bodies are seaward of the Sigsbee in the vicinity of GC 955. One of them, Green Knoll, is a large salt diapir, once thought to be isolated (Swiercz, 1991), but now understood to be connected to the mother salt by a salt stock (Kendall, personal communication). Green Knoll is approximately 8 to 10 miles in diameter with 1850 ft of relief relative to the surrounding seafloor, approximately six miles to the east of GC 955 (Figure F5). The other salt body is an allochthonous, hourglass-shaped (in plan view), shallow salt body trending southwest to northeast from WR 30 to GC 955 that is connected by a salt stock to the deeper mother salt beneath the Sigsbee front to the northeast (Kendall and Pilcher, personal communications) (Figure F5). The shallow salt body has uplifted sediments, forming keystone faults that extend within a few hundred feet of the seafloor in southern GC 955 (Figure F6). The salt bodies in the local area all strongly contribute to faulting and impact the fluid flow dynamics to the target gas hydrate sands.

Conventional oil and gas exploratory efforts have identified petroleum systems in the GC 955 block that resulted in three wells, GC 955 #001, GC 955 #002, and a sidetrack delineation well from the GC955#002 location. GC955#001, drilled by Statoil USA in 1998, was an exploratory well targeting potential hydrocarbons in the Plio-Pleistocene sediments forming traps against salt. Hydrocarbons, if found, were not in quantities deemed to be commercial and the well was plugged and abandoned. Kerr-McGee, later to become part of Anadarko, drilled the GC 955 #2 well in 2006 that discovered oil in sub-salt mid-Miocene sediments (Anadarko, 2006). Further delineation of the reservoir from the GC 955 #2 location was completed by Anadarko in 2008.

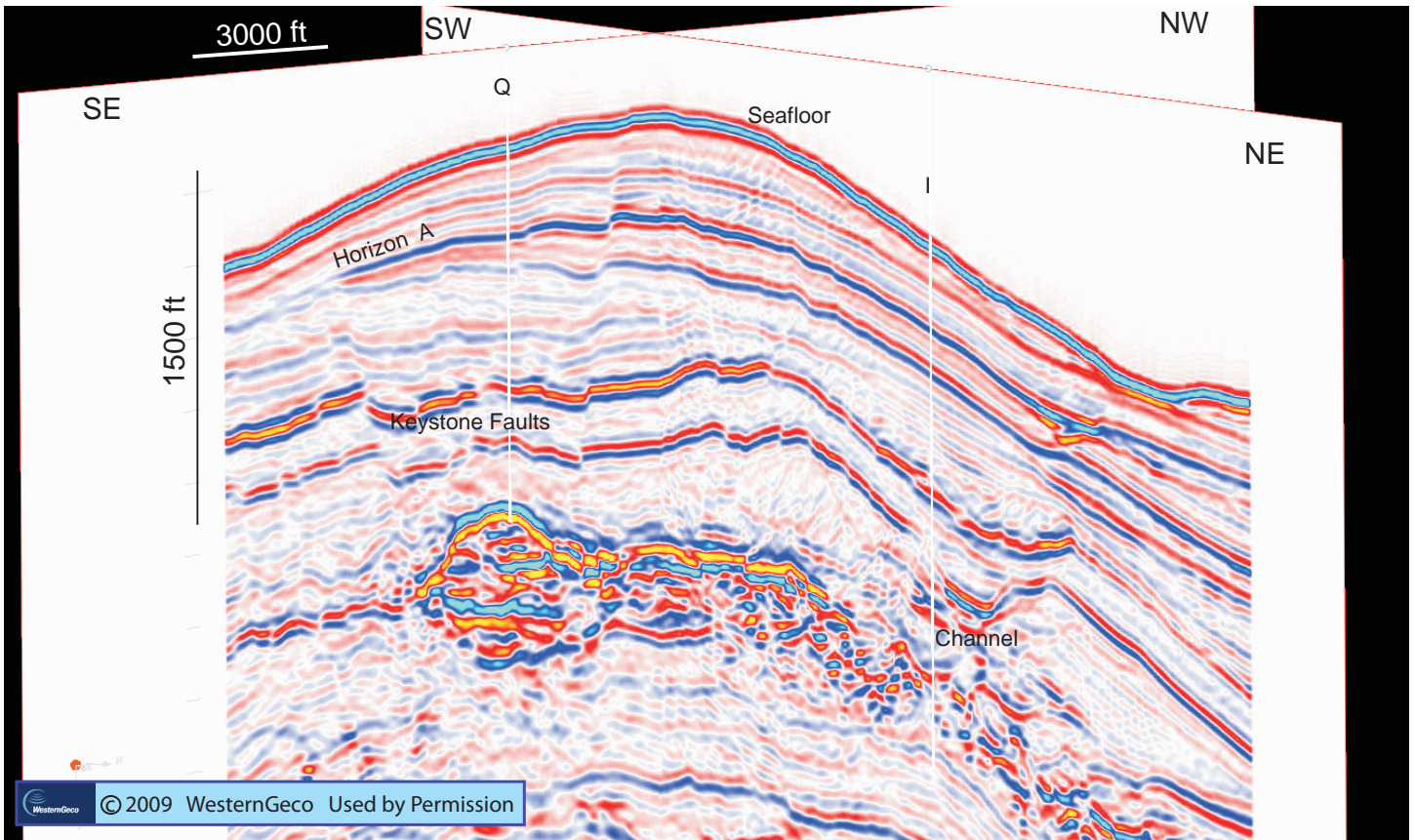


Figure F4: Perspective view from 3-D seismic of keystone faults on SE-NW traverse and high amplitudes suggesting mixed gas hydrate and gas along the projected freeze line and relationship to channel facies. Traverses are coincident with the Q and I wells. Background seismic data courtesy of WesternGeco.

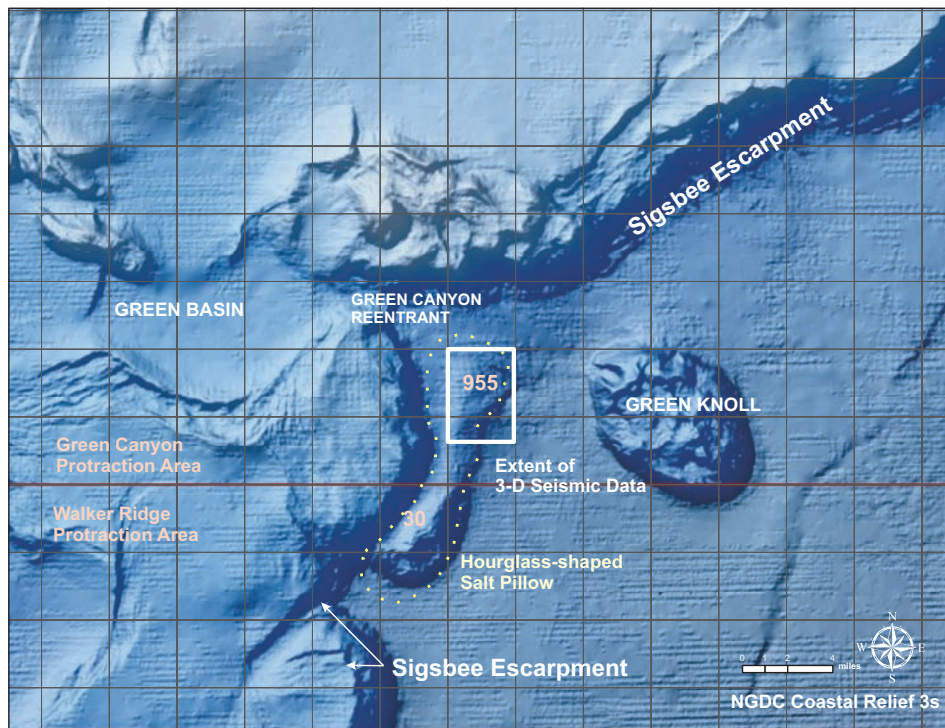


Figure F5: Green Canyon re-entrant on the Sigsbee Escarpment showing Green Knoll, hourglass-shaped salt pillow beneath GC 955 and WR 30, and extent of 3-D seismic data.

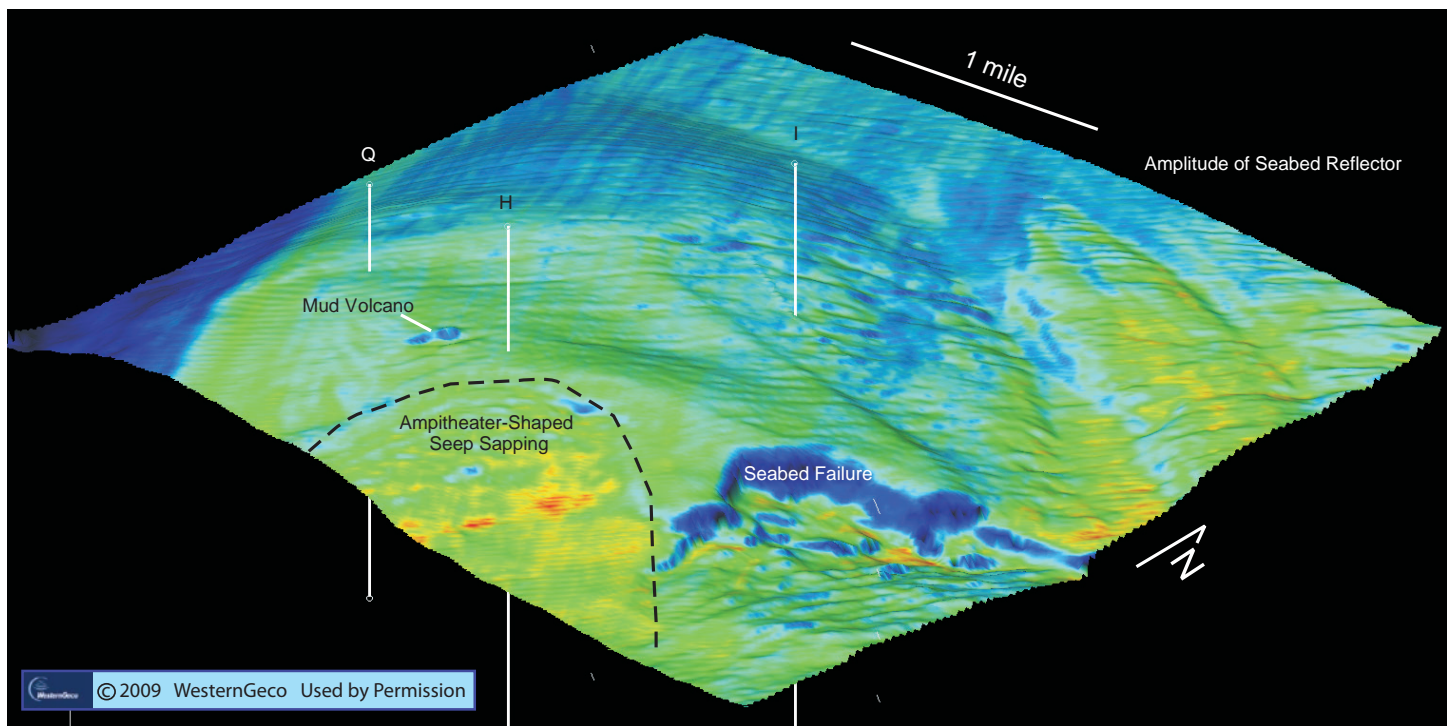


Figure F6: Perspective view from 3-D seismic of seafloor amplitude showing JIP wells and evidence of fluid flow to seabed. Image courtesy of WesternGeco.

Gas and Fluid Sources and Migration Pathways

Extensional faults extending from the shallow salt body in GC 955 into the gas hydrate stability zone are interpreted to be conduits for fluids, including gas, to move through the shallow sediments. On southwestern and southern flanks up the uplift, there are three “horseshoe-shaped” escarpments showing seafloor failure (Figure F6). Orange *et al.* (2003), showed similar features in the “Mad Dog” development area 16 miles to the northeast, and interpreted that they were caused by internally driven failure by fluid flow and gravity processes at overpressured sand cropping out at the base of the Sigsbee Escarpment face. The amphitheatres form by seepage along the shortened flow paths at the aquitard (a layer that impedes but does not prevent fluid flow) (Orange, 1992). A similar mechanism for fluid flow, albeit on a smaller scale, is recognized in the “horseshoe-shaped” seabed morphology and shallow subsurface sediments in GC 955, that suggest imminent and recent seafloor failures caused by internally driven failure rather than by oversteepening alone. In GC 955, most of the faults extend to Horizon A (Figure F4), about 315 feet below the seafloor (fbsf) at the crest of the uplift. Horizon A, acting in a similar way to the failure models at the Sigsbee face, also marks the base of the seafloor failure in the SE quadrant of the lease block. Heggland (2004) noted fluid flow into the

shallow sediments through gas chimneys identified in the seismic data and the seafloor failure. A mud volcano at the seafloor above one of the buried faults is further evidence that fluids move through the sediments to the seafloor (McConnell, 2000; Heggland, 2004). This evidence for fluid migration in addition to the high-negative impedance gas and high-positive impedance gas hydrate anomalies centered above the crest of the shallow salt in the faulted sediments (discussed below) strongly suggests fluid flow through the shallow sediments. Fluid migration along the faults is also strongly suggested by the prominent seismic anomalies indicative of gas in the faulted four-way closure that prompted the search for gas hydrates in the block.

Reservoirs

The shaded relief bathymetry map shows the complex seafloor topography in the tabular salt and mini-basin province (Figure F1). At lowstand, numerous Late Pleistocene sediment fairways extended from the shelf edge to the continental slope. Nibbelink (1999) shows several channel sands and perched sands on the upper part of the escarpment. Similar sediment fairways extend from the shelf edge, across the mini-basin province, some through Green Canyon proper, past the Sigsbee Escarpment and onto the continental rise. Detailed mapping of the Pliocene and Pleistocene Mississippi Fan seaward of the Sigsbee

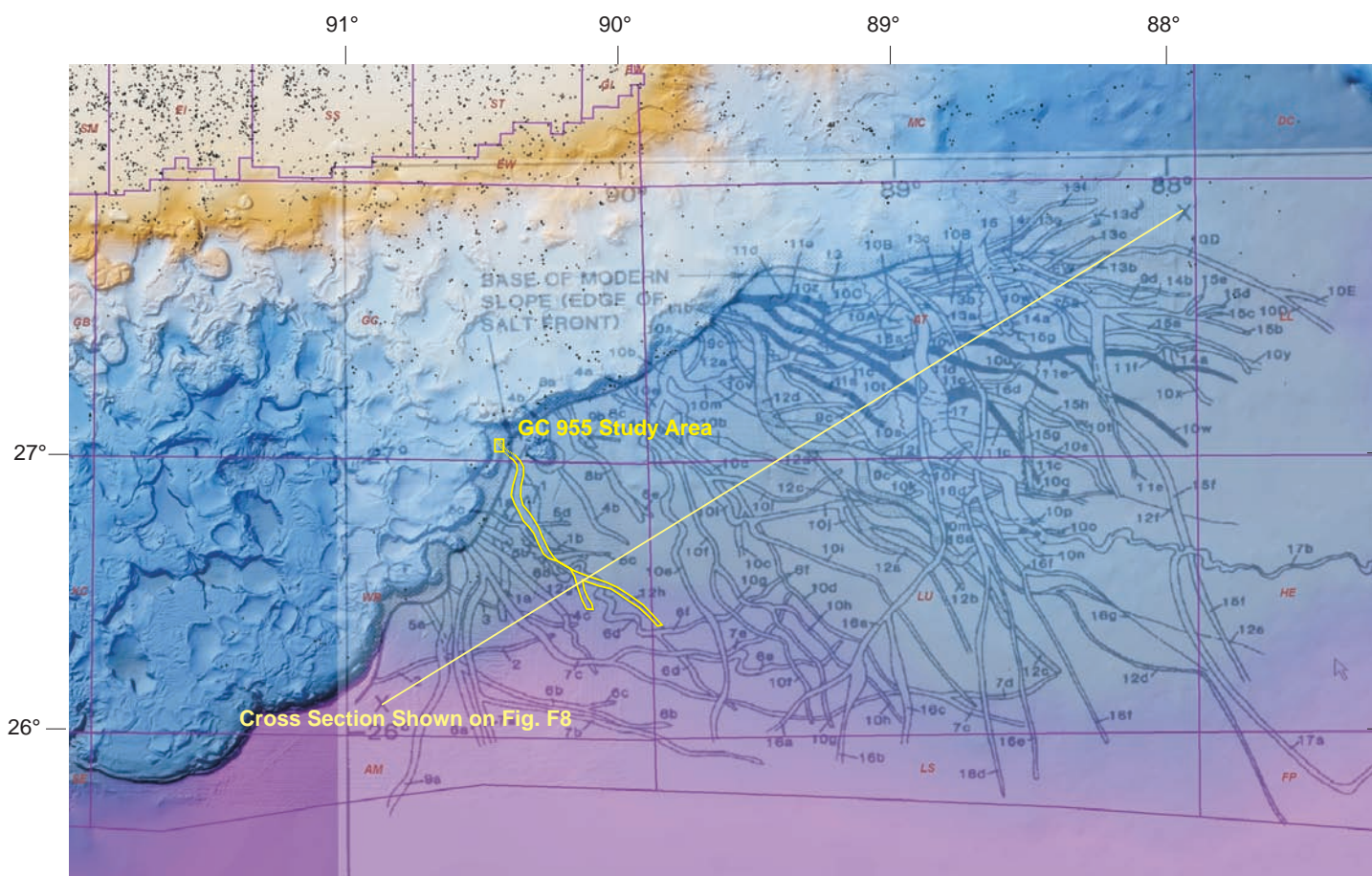


Figure F7: Overlay of Weimer, 1990, Mississippi Fan channel valleys over NGDC 3s bathymetry data showing Channel 12h and 12g (in yellow) associated with gas hydrate target facies in GC 955.

escarpment shows sand-prone channels and channel-levee systems interbedded within the thick (>4 km) mud-dominated Mississippi Fan (Weimer, 1990; Figures F7 and F8). The large channel and channel levee system sands targeted for drilling by the JIP corresponds to Weimer's channel-levee **system 12** of the 17 channel-levee systems (1 is oldest, and 17, youngest) comprising the Mississippi Fan (Figure F8).

As it traverses GC 955, the top of channel-levee complex 12 is approximately 1000 fbsf and the channeled interval, including channel fill sediments is in excess of 700 ft thick. The prominent late-stage channel is approximately 1.3 miles across from levee crest to levee crest. Biostratigraphic data collected during drilling of the GC 955 #001 well is not yet public, but is scheduled to be released in 2010. However, Weimer (1990; citing Walters, 1985), estimates the age at the top of channel-levee system 12 at 0.5 Ma.

Because the most clearly imaged channel axis within this channel-levee system (Figures F2 and F9) occurred off the flank of the prospective structure (and therefore away from the focus for gas and fluid flow above the shallow salt), the drilling targets on this structure were assessed to be at increased risk of penetrating lower quality and thinner sands than observed in the GC 955 #001 well (Hutchinson *et al.*, 2009).

Geophysical Indications of Gas Hydrate

In addition to exhibiting indications of gas supply, migration pathways, and reservoir into and within the GHSZ (all components conducive to hydrate formation), several features are observed at GC 955 which suggest the presence of gas hydrate. First among these is the occurrence of strong amplitudes with clear "leading peaks" (strong positive-polarity reflectors). Such reflectors, where they exist within the potential GHSZ and within intervals expected to be sand prone, are highly prospective for high concentrations of gas hydrate (McConnell and Zhang, 2005).

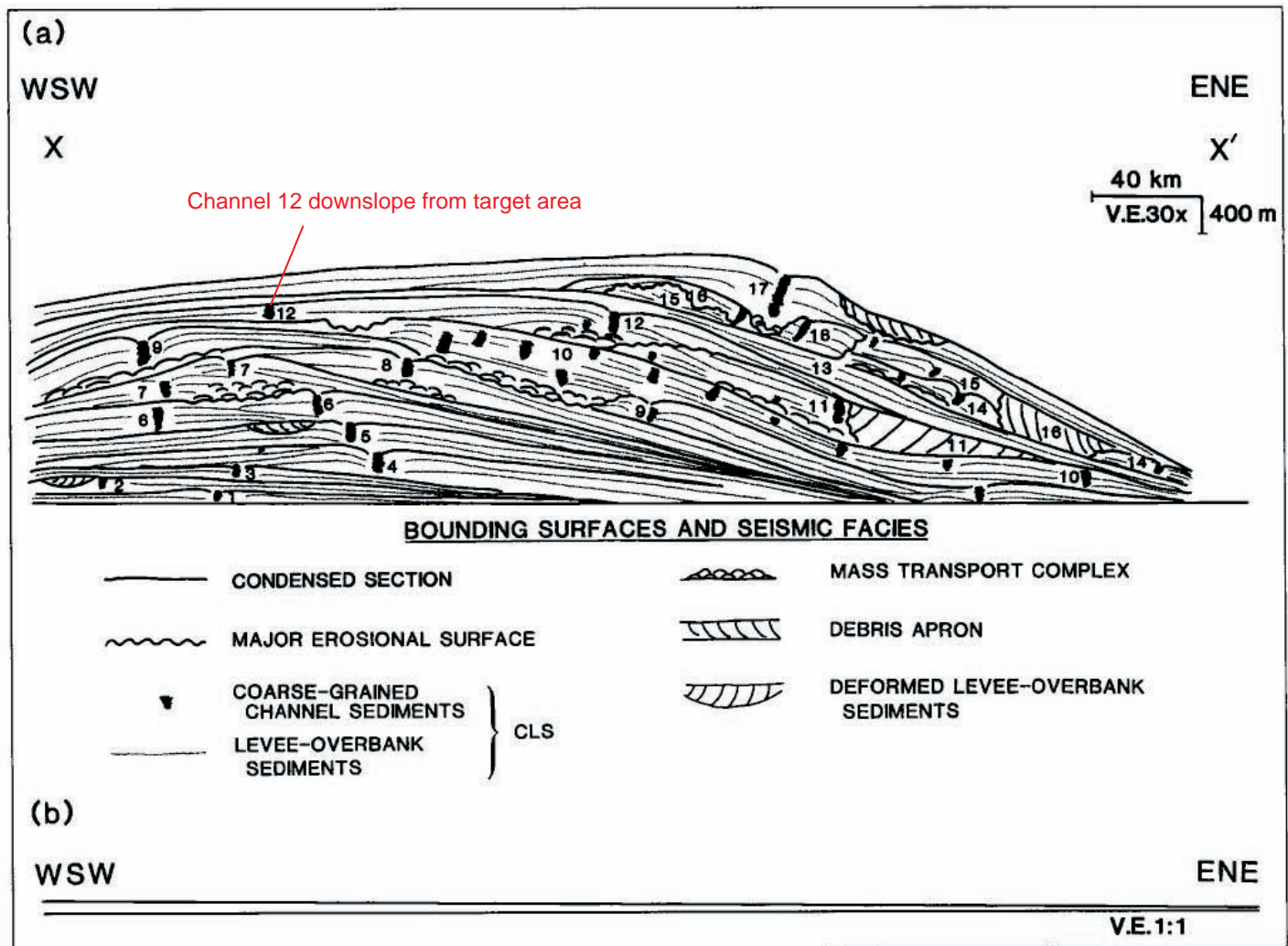


Figure F8: Cross-section showing cross-section of Mississippi Fan. Channel 12 associated with gas hydrate-bearing sediments in GC 955 is illustrated (modified from Weimer, 1990).

Analysis of the seismic data from the block also shows that such reflectors, while highly patchy and discontinuous, are most common in the area of the closed structure (Figures F2, F4, and F9). A second indication of gas hydrate is the anomalous trend of apparent gas trapping within the closure. Despite the presence of numerous fault-related pathways and the expected porous and permeable strata in directly overlying unit, gas (as indicated by strong negative impedance amplitudes) is restricted below a horizon of relatively consistent sub-seafloor depth with no clear geologic explanation. The occurrence of this “pseudo-bottom simulating reflector (BSR)” within the sand-prone section suggests that the migrating fluids are forming gas hydrate at the stability boundary, and restricting further upward gas migration (Shedd *et al.*, 2009). This phenomena is recognized as being complex, with numerous high amplitude reflectors of both positive and negative polarity

occurring in close association, suggesting a mixed gas and gas hydrate system within the sand in the four-way closure.

GC 955 Gas Hydrate Prospect Models

The primary gas hydrate prospects identified by the site selection team all trend near the base of gas hydrate stability in a local area of high fluid flux within or near the four-way closure. In the prospect model for these locations, fluids oversaturated with gas move vertically along faults and fractures (with a potential lateral fetch component from fluids moving along the salt face at the Sigsbee escarpment 6 miles to the north and along the salt stock connecting the shallow salt body to the mother salt to the west) into thick sands spanning the gas hydrate stability field. This gas then converts to gas hydrate within the sand along a relatively thin layer at the base of the stability zone. Other potential mechanisms for gas hydrate emplacement, such as *in situ* gas methane hydrate production, upward

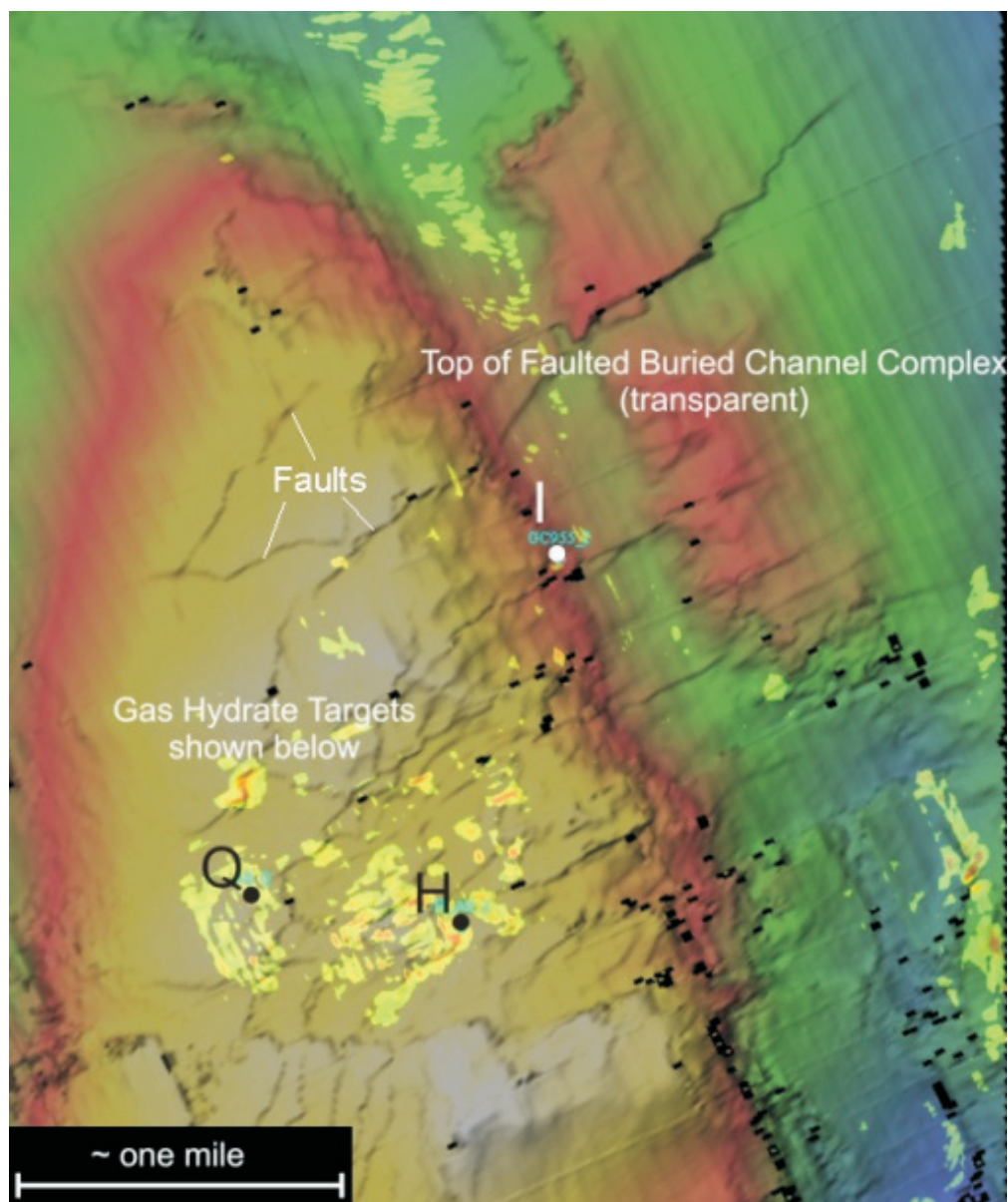


Figure F9: Top of channel facies (transparent) showing gas hydrate targets below and JIP well locations. Image and data provided by Western Geco and Schlumberger.

diffusive flux and exsolution, and concentration by recycling of low concentration gas hydrate in response to sedimentation, were not considered in the pre-drill determination of the primary drilling targets. Where this zone of basal hydrate accumulates to sufficient thickness to be seismically resolvable (either due to continued sourcing or due to subsequent lowering of the BGHS), a strong peak reflector is produced at the top of the highly-concentrated gas hydrate occurrence. This model was considered the most likely case for those prospects within the structural closure. However, given the interpretation of contiguous sand reservoir extending much further up in the section, the GC 955 Site afforded the opportunity to test two lower-

probability but intriguing hypotheses. In one alternative model, gas hydrate extends above the peak reflectors but in low or in steadily decreasing concentrations (perhaps tied to reduced and decreasing upwards reservoir quality, a reasonable possibility for channelized deposits) such that no interfaces of sufficient impedance contrast are produced. Second, gas hydrate extends above the peak reflectors, but is limited to areas very close to the primary fault migration plains, hence creating gas hydrate units with high-angle orientations that are not readily resolved in the seismic data.

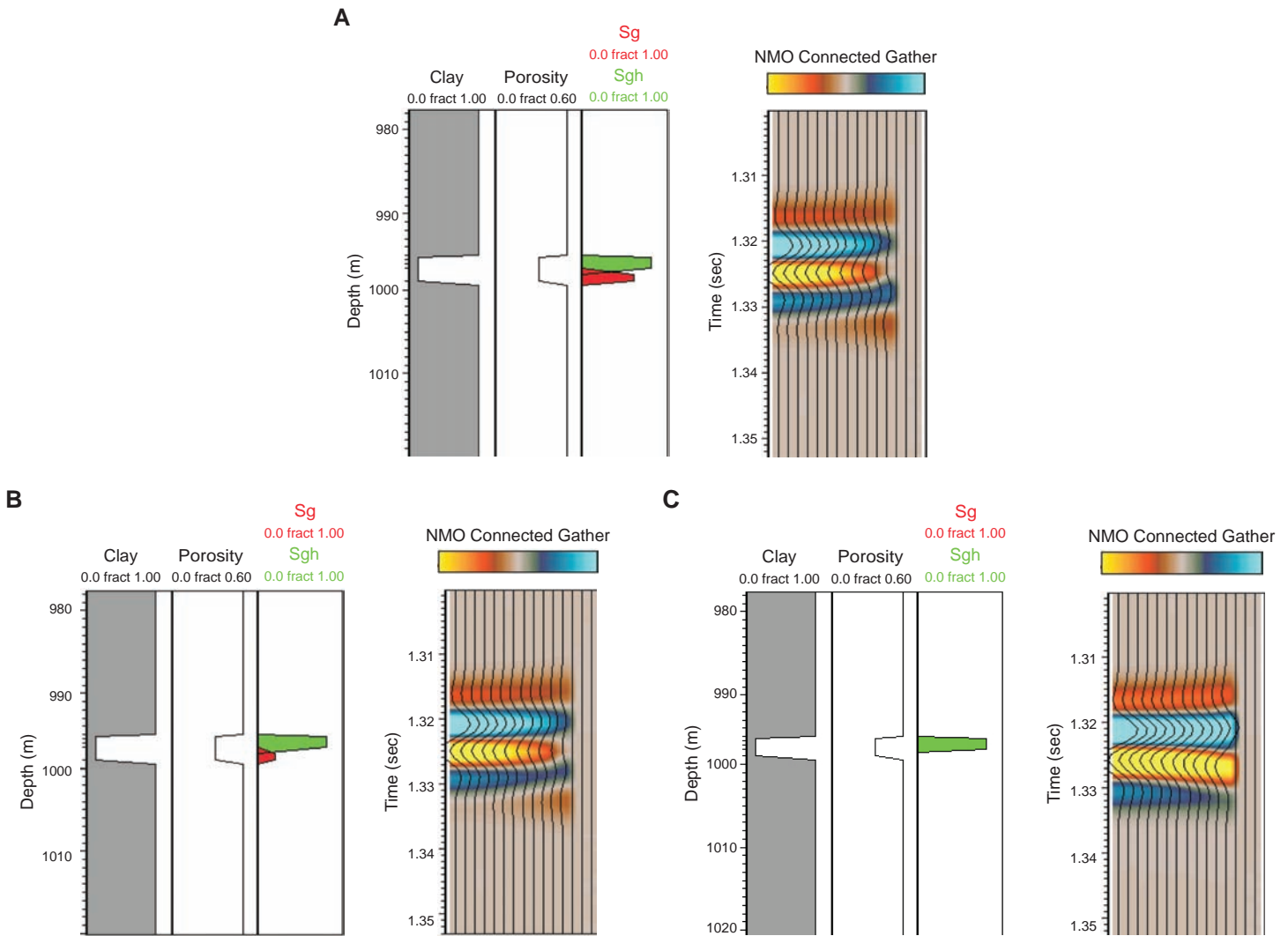


Figure F10: Synthetic gathers showing response of various concentrations of gas hydrate (green) over gas (red) as might be found at the base of gas hydrate stability (modified from Nur and Dvorkin, 2008).

Shallow Hazards Analysis

The risks of shallow drilling hazards to personnel during riserless deepwater drilling operations are negligible. However, geohazards, such as gas and water flows, can require significant time to properly control. For a project such as the JIP, which is constrained to a set budget and time period, significant lost time translates directly into undrilled holes and uncollected data. In addition, JIP Leg II deployed one of the most advanced and expensive LWD tools strings ever assembled. Issues such as a loss of borehole stability that can result in damaged, even lost tools, must be very carefully evaluated and managed. Because all of the potential holes considered by the JIP were to be drilled open hole (without casing, risers, or blow-out preventers), the options available for management of well problems were limited to the use of weighted mud and cement. Therefore, to minimize the chances for costly downtime, the

JIP ordered a thorough geohazards and wellbore stability analysis for all potential sites, even though regulations did not require that level of analysis in every case.

In order to provide optimal data throughout the section of interest, each planned well depth extended to 500 ft below the base of predicted gas hydrate stability. Therefore, one of the principal hazards in GC 955 was the potential for gas flows from free gas zones in the bottom of the holes. Another key issue was the potential for slight overpressures that can cause water flows and/or wellbore collapse in the unconsolidated marine sediment. The pre-drill hazards analysis evaluated all potential holes in GC 955 for these risks and moved or eliminated potential locations as required. This work was particularly critical for those locations on the structural high where free gas indicators (strong “trough” amplitudes) were commonly

JIP Leg II Well	Latitude NAD1927: Clarke	Longitude NAD1927: Clarke	Water depth (ft)	Total depth (fbrf)
GC 955-I	27 00 59.5305 N	90 25 16.8928 W	6770	9027
GC 955-H	27 00 02.0707 N	90 25 35.1142 W	6670	8654
GC 955-Q	27 00 07.3484 N	90 26 11.7156 W	6516	8078

Table T1: Information on the three wells drilled in GC 955.

associated with (directly underlying) the most promising gas hydrate indicators. However, due to the weak sensitivity of seismic amplitude to free gas saturation, it is not possible to confidently determine if such paired peak-over-trough signatures represent gas hydrate over water or gas hydrate over free gas (see Figure [F10](#); after Nur and Dvorkin, 2008). The hazards work therefore assumed such events represented potential gas flow hazards. The primary hazards mitigation strategy was to locate wells where the “trough” amplitudes could be avoided or penetrated in locations with minimal downdip reservoir extent. Overall, eleven possible locations in GC 955 were ranked for shallow hazards. Generally, those with the less prospective hydrate potential, such as those with targets well above the inferred BGHS or those located off the structure, away from the strongest amplitudes, were assessed with the lowest shallow hazard risks.

GC 955 Drilling Results

Three holes, locations I, H, and Q, were drilled at the GC 955 Site (Table [T1](#)). The rationale for the selection of these sites from among the 11 permitted sites is described in Boswell *et al.* (2009). An arbitrary seismic traverse showing the drilled locations and the industry wells is shown as Figure [F11](#) and as Figure [F12](#) with gamma ray and resistivity log overlays. The predicted gas hydrate saturations along the same traverse are shown as Figure [F13](#) and with gamma ray and resistivity log overlays as Figure [F14](#). The same traverse is shown in the results obtained from the three wells drilled during the program. These wells are described in Table [T1](#).

Well GC 955-I

The GC 955-I location was drilled off the structural closure in a location proximal to both the pre-existing GC 955 #001 well and the primary imaged channel-levee axis. The primary target at the I-location was a muted peak amplitude anomaly 320 ft above the interpreted base of gas hydrate stability. The amplitude was stratigraphically correlative to a 4 Ω -m resistivity anomaly logged in the #001 well interpreted to represent up to 15 ft of gas hydrate within

the middle of a 520-foot thick sand section (Figure [F12](#) and [F14](#)). Given its proximity to both the #001 well and the channel-levee axis, the I-location was assessed with a high probability of encountering clean sand within the GHSZ. In addition, the location of the primary geophysical indicators relative to the BGHS and lack of strong amplitudes resulted in a low risk for gas flows. The pre-drill gas hydrate saturation prediction at the GC 955-I hole from the seismic inversion analyses conducted by WesternGeco ranged from 28% to 69% over a small area around the well location, with most values above 45% (Hutchinson *et al.*, 2009).

In general, the quality of the downhole log data acquired from the GC 955-I well was high to good (Guerin *et al.*, 2009). For the most part, caliper data show that the hole was in gauge when logged except for within a sand-rich interval from ~1240 fbsf to ~1620 fbsf, which exhibited “wash-outs” on the caliper log measuring about 1-2 inches larger than the drill bit (8.5 inch hole).

The sediments logged in the GC 955-I well can be generally divided into three major stratigraphic sections, with the sedimentary section from the seafloor to a depth of ~1240 fbsf characterized by uniform gamma-ray values of 75 API, indicative of a mud-dominated sediment. From ~1240 fbsf to 1620 fbsf, gamma-ray log values are highly variable with values ranging as low as 20 API indicative of an interbedded shale and sand section with individual sand beds ranging in thickness from about 1-2 ft to as much as 10 ft and greater. This sand-prone section consists of three primary sub-units: a basal unit denoted by generally decreasing gamma-ray, a 35-ft thick shale-rich middle unit containing only a few thin sands (from 1535 fbsf to 1570 fbsf), and an upper sand section with sharp basal contact and a generally shaling-upward structure. The section below ~1620 fbsf appeared to be dominated by fine-grained sediments to the bottom of the hole. The resistivity log from the GC 955-I well is very uniform over the entire well with values ranging from ~0.7 Ω -m in the sand units to 1.5 to ~2.0 Ω -m in the shale sections (Figure [F15](#)). For the most part these

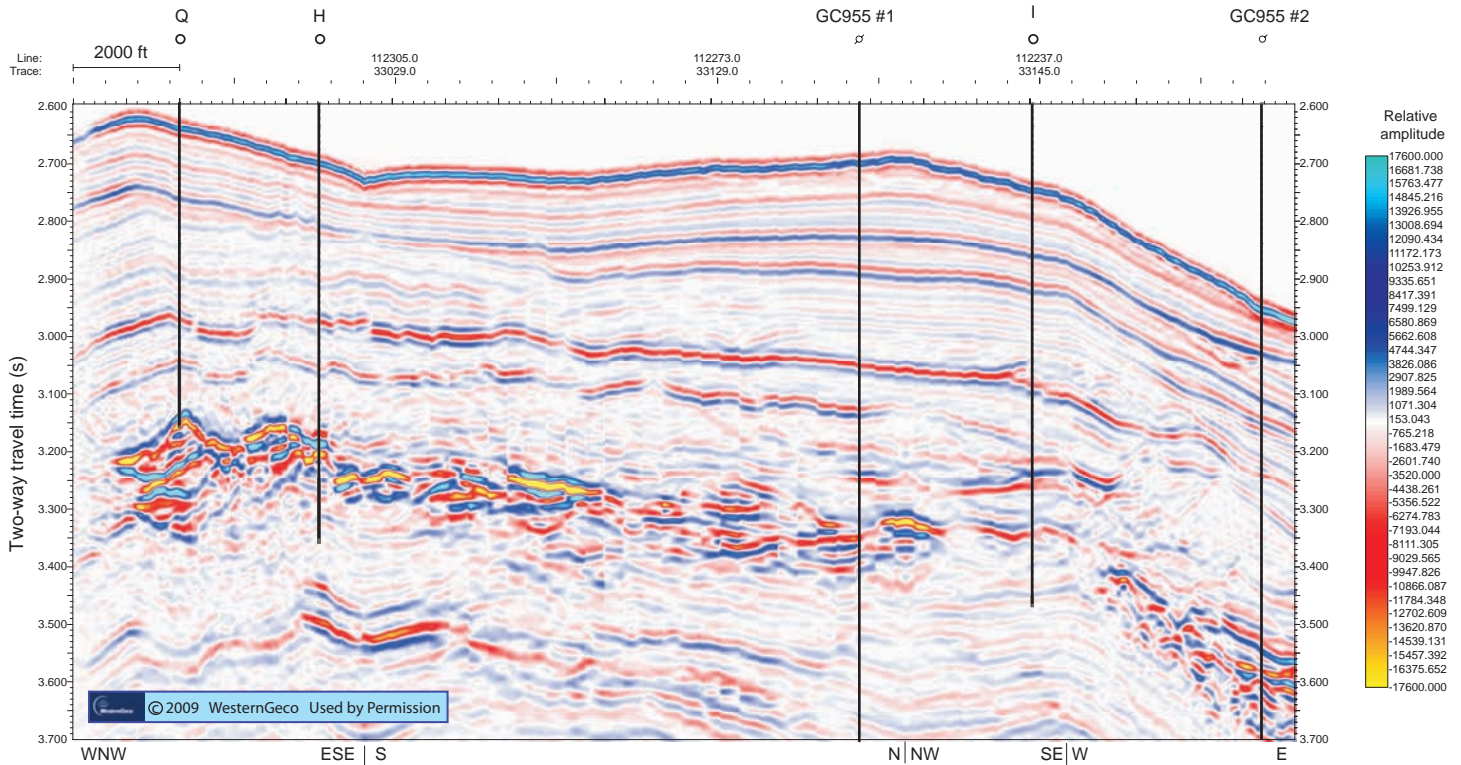


Figure F11: Arbitrary line through amplitude volume showing JIP and industry wells. Seismic data courtesy of WesternGeco.

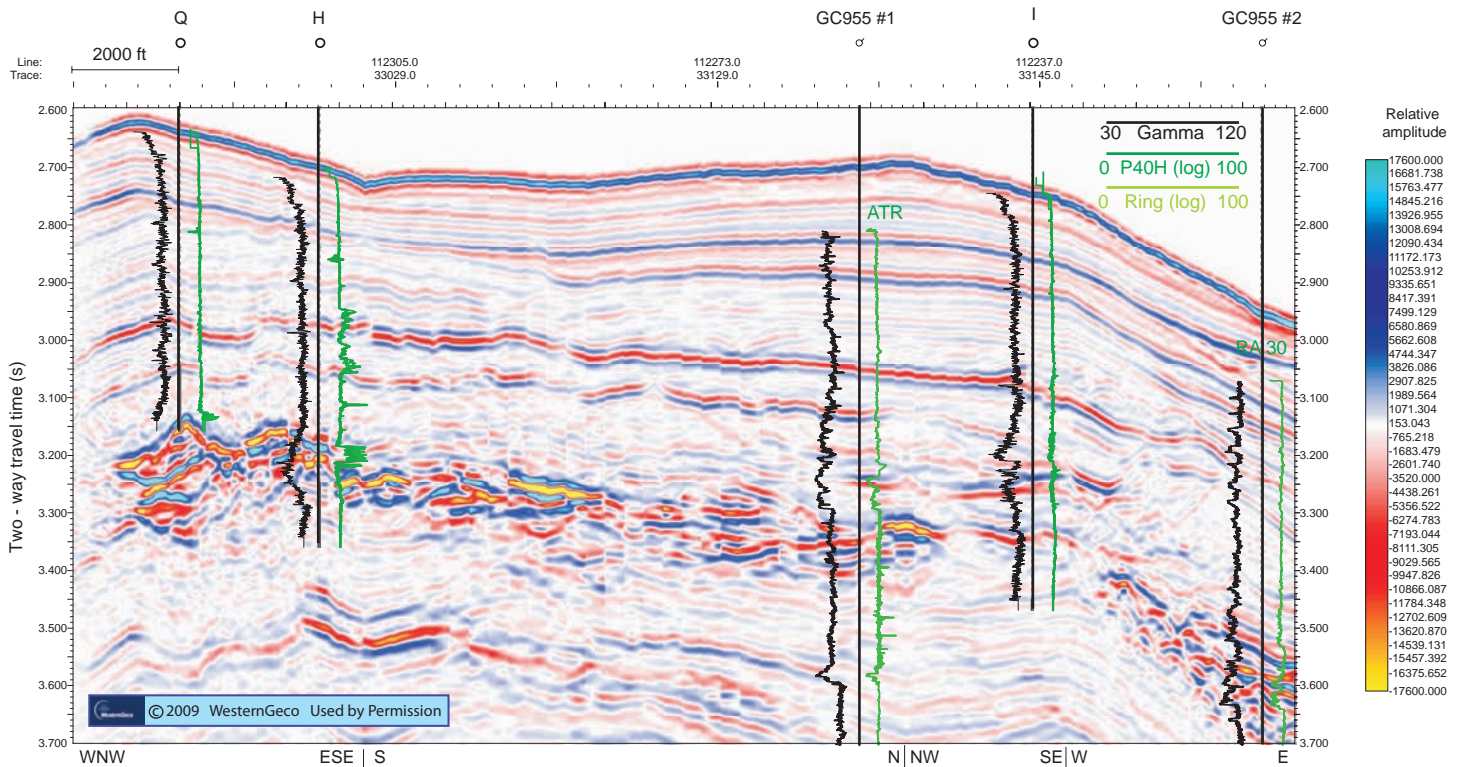


Figure F12: Arbitrary line through amplitude volume showing JIP and industry wells with gamma and resistivity logs. Seismic data courtesy of WesternGeco.

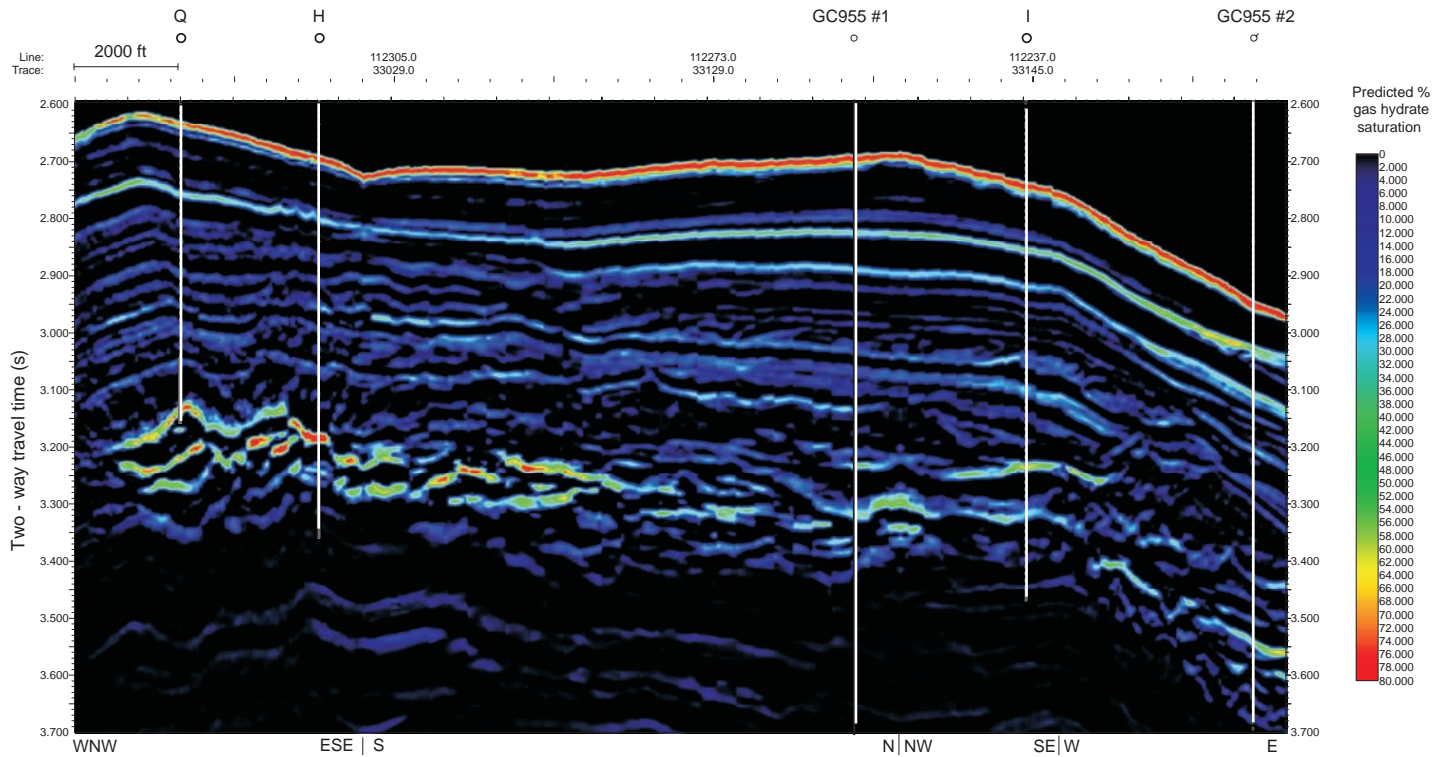


Figure F13: Arbitrary line through gas hydrate saturation prediction volume showing JIP and industry wells. Hydrate saturation data provided by Schlumberger.

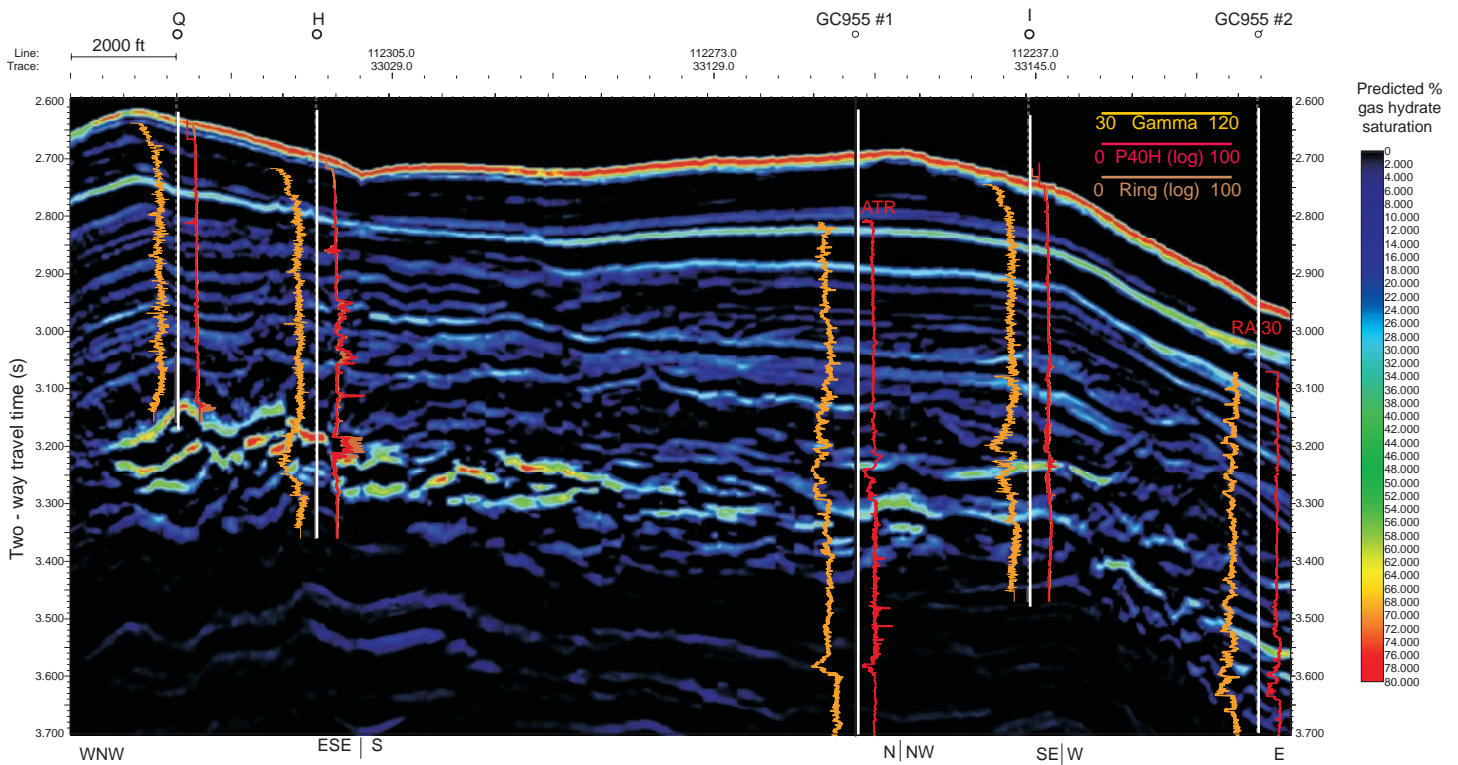


Figure F14: Arbitrary line through gas hydrate saturation prediction volume showing JIP and industry wells with gamma and resistivity logs. Hydrate saturation data provided by Schlumberger.

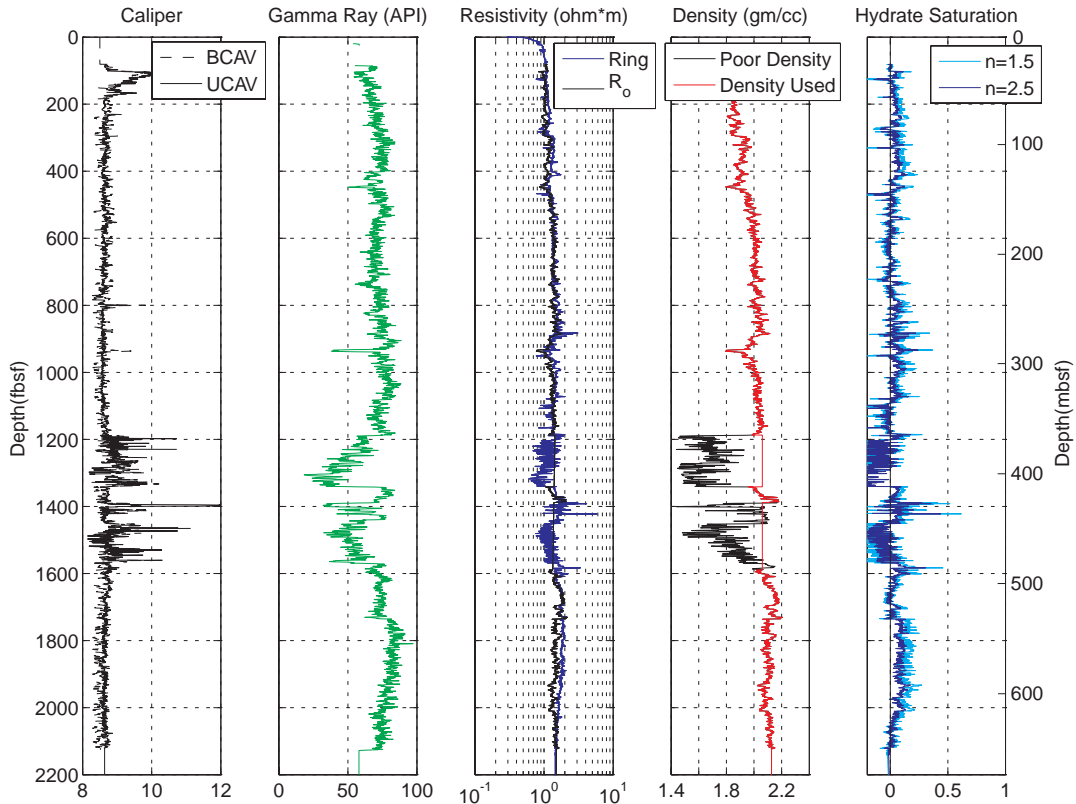


Figure F15: Caliper, gamma, resistivity, density, and hydrate saturation logs at Well GC 955-I (Guerin et al., 2009).

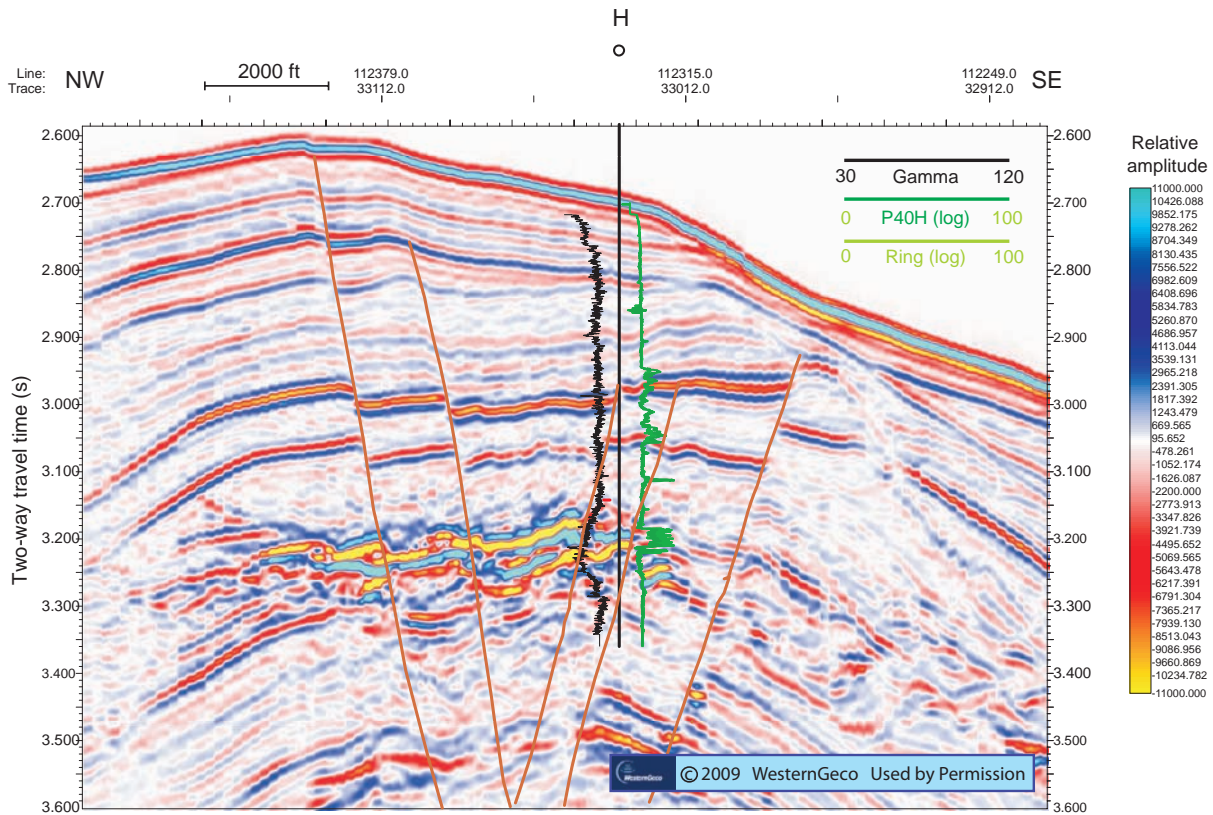


Figure F16: Arbitrary line through amplitude volume showing faults and Well GC 955-H with gamma and resistivity logs. Seismic data courtesy of WesternGeco.

low resistivity log values indicate the presence of water-bearing sediments (i.e., no gas hydrate or free-gas). The only evidence of elevated resistivity (3 to 5 Ω -m) occurs within a few feet of sand within the middle shaley portion of the sand unit. These elevated resistivities directly correlate with high velocities of 2290 m/s and 2190 m/s and initial S_h estimates as high as 50% (Guerin *et al.*, 2009). Upon removal of the tool string from the hole, a small flow of water was observed at the seafloor by the Q-4000's ROV which required nearly a day of effort to control (Collett *et al.*, 2009).

Well GC 955-H

The GC 955-H well targeted an anomalous seismic peak over strong trough in the interpreted sand facies. The location is on the flank of the structural closure, in a location downthrown and to the east of a large normal fault (Figure F16). The location was assessed with a high probability of encountering sand in the GHSZ and a moderate risk for free gas just below the gas hydrate target. Seismic inversion analysis indicated high potential for gas hydrate of at least 50% saturation in an area at least 1500 ft by 2800 ft (0.12 sq miles) in size. The H location targeted the strongest amplitudes, corresponding to a pre-drill gas hydrate saturation prediction from seismic inversion analysis of at least 95% (Hutchinson *et al.*, 2009).

Drilling at GC 955-H revealed a shale-rich section extending from the seafloor to a depth of ~1275 fbsf. Within the upper shale section, resistivities gradually increase to about 1.5 Ω -m at 625 fbsf. From that depth to ~965 fbsf, resistivities are highly variable, ranging up to 4 to 10 Ω -m (Figure F17 and F18). Elevated compressional velocities of 1905 m/s correspond with the 3.6 Ω -m resistivity anomaly between 703 and 730 fbsf within and above a thin sand interbed. Between 887 and 957 fbsf, the 6 to 10 Ω -m shaley section does not correspond with anomalous compressional velocities, although the velocities appear to be elevated above trend. Azimuthal resistivity images indicating the occurrence within highly-inclined resistivity fractures indicated grain-displacing gas hydrate occurrence (Figure F19, Guerin *et al.*, 2009). No clear evidence was found to support the hypothesis that gradually decreasing gas hydrate might be present in sands above the target peak reflector but the highly inclined resistive sections correspond to intervals where several seismically-imaged faults are interpreted to intersect the borehole.

From 975 fbsf (the base of the fracture-filling gas hydrate zone) to the top of the sand section at 1275 fbsf, resistivity varies across a range from 1.5 to 3 Ω -m. Where there are thin sands, between 997 and 1010 fbsf, elevated compressional velocities of 1917 m/s correspond with the 3 Ω -m resistivity. From 1275 fbsf to 1600 fbsf, gamma-ray values are generally lower, indicating a 325-foot thick sand section. The sand is highly-gradational at both top and base. Resistivity in the unit is highly variable. For the upper 80 ft of the unit, resistivities steadily decline to ~0.8 Ω -m. There is then an extremely sharp contact, despite lack of evidence for any major lithologic variation, and resistivities climb to ~20 Ω -m or greater and compressional velocities sharply increase from 1675 m/s to 2458 m/s. For the next 86 feet (from 1358 to 1444 fbsf), resistivities range from ~20 to ~200 Ω -m corresponding with high compressional velocities between 2540 and 3110 m/s (Figure F20). Gamma values indicate that the unit consists of numerous thin (1 to 3 ft) interbeds in this section (Figure F20). At 1444 fbsf, resistivities again abruptly drop to as low as 0.5 Ω -m indicating a sharp change in pore fill, again with no clear lithologic control. This apparently water-bearing interval extends to 1457 fbsf – at that level resistivities again abruptly increase and vary from 6 to 30 Ω -m with corresponding high compressional velocities of 2650 m/s. This second resistive interval is ~9 feet thick, and directly underlain by another low-resistivity unit ~4 feet thick. At 1475 fbsf, a third resistive unit (~10 to 15 Ω -m), ~3 feet thick, corresponding with high compressional velocities of 2400 m/s, was logged. From the base of this unit to the base of the sand at ~1600 fbsf, resistivities are low, ranging from 0.7 to 1.5 Ω -m. The section is predominately fine-grained from 1600 fbsf to the bottom of the hole.

This combination of high resistivity and high compressional velocity indicates likely high concentrations of gas hydrate pore fill (Figure F18). Significant additional work will be required to understand the nature and controls on this occurrence, particularly the alternating occurrence of gas hydrate and water pore fill within an apparently single sand reservoir. In addition, there was no indication of any appreciable volume of free gas in the ~100 feet of sand reservoir underlying the deepest gas hydrate occurrence in this well. Consequently, the strong trough event noted on the seismic data was driven largely by the juxtaposition of hydrate over water.

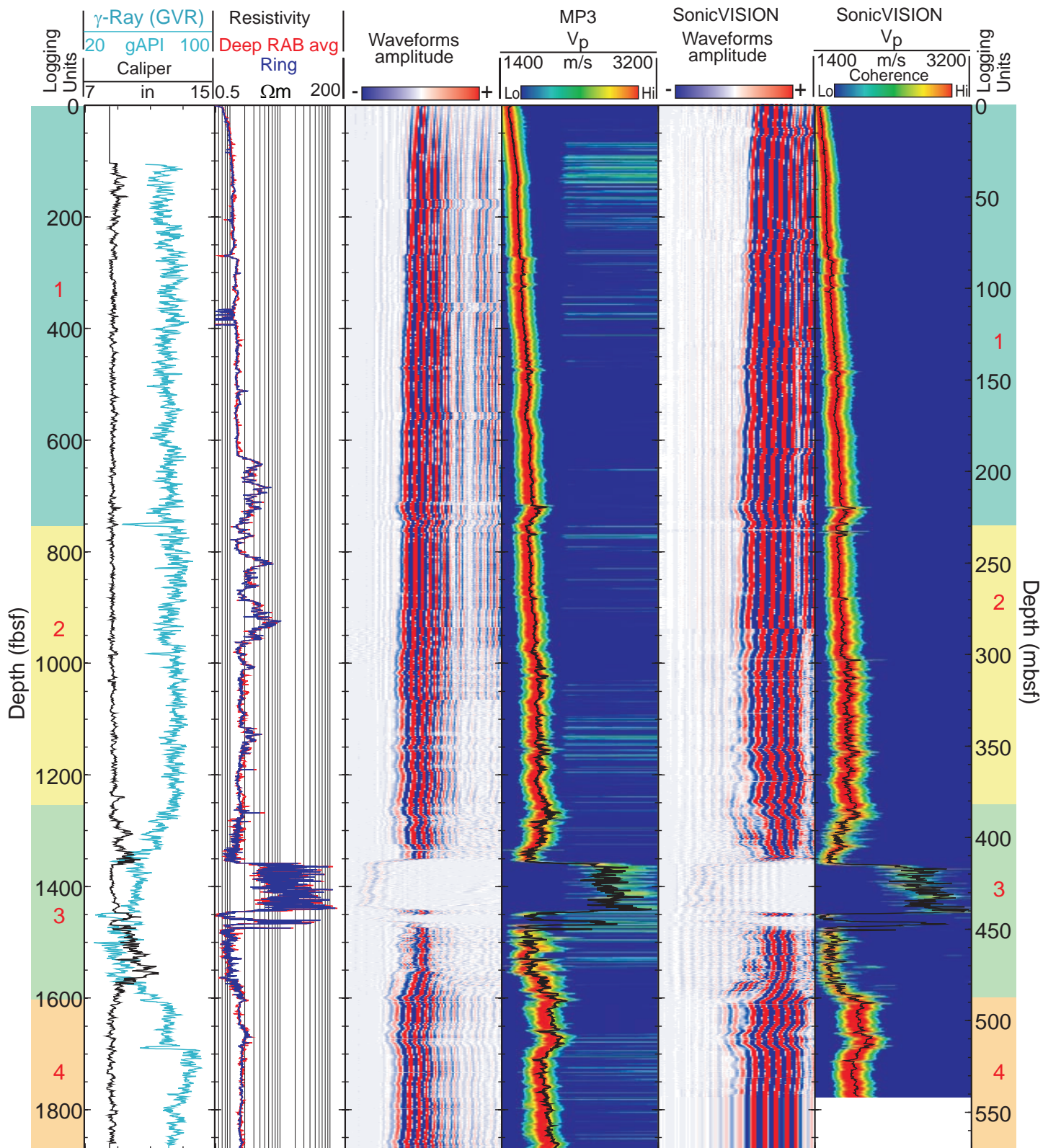


Figure F17: Gamma, resistivity, and sonic logs at Well GC 955-H (Guerin et al., 2009).

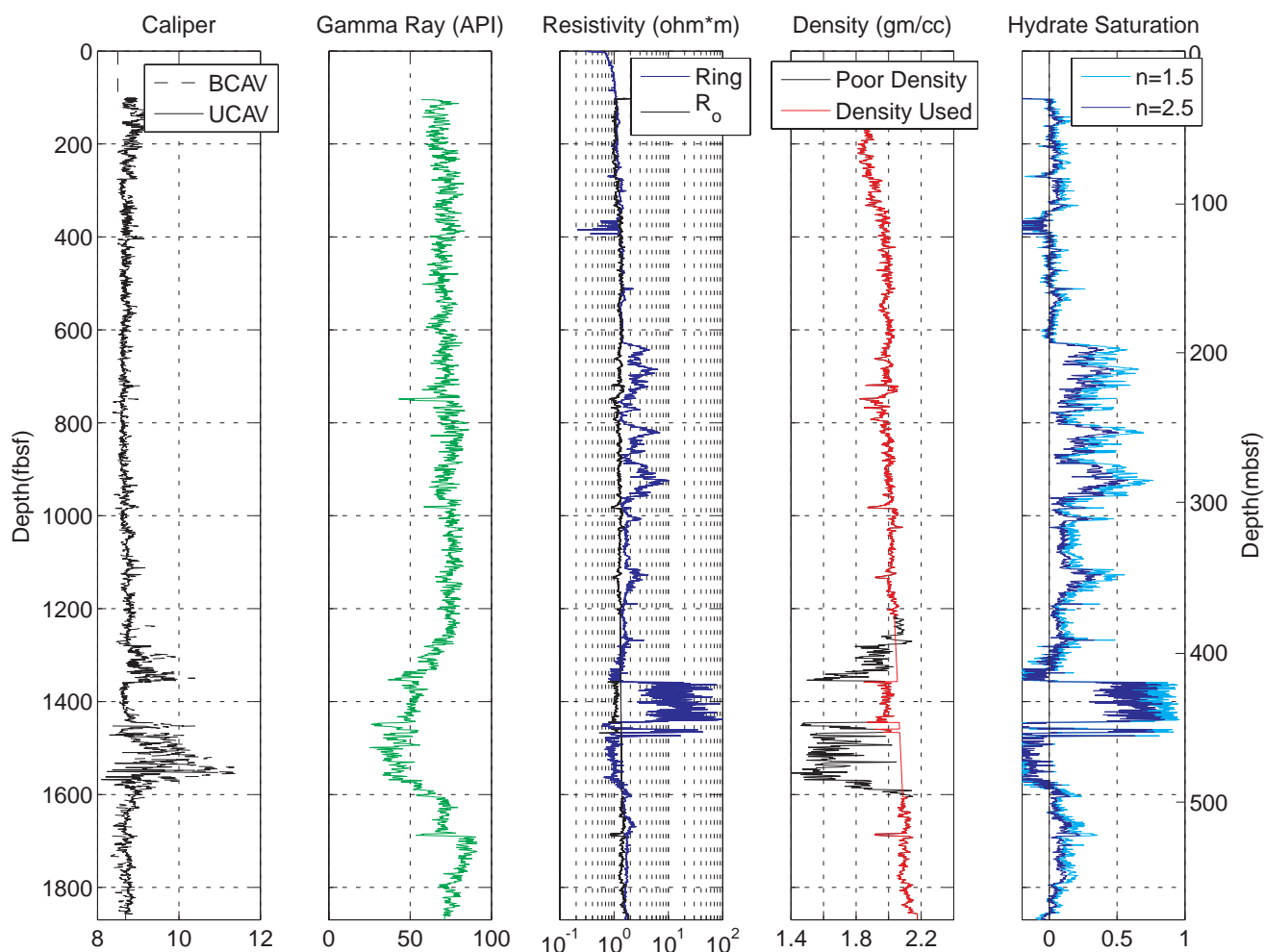


Figure F18: Caliper, gamma, resistivity, density, and hydrate saturation logs at Well GC 955-H (Guerin et al., 2009).

Well GC 955-Q

Based on the drilling results at the GC 955-H well, the science team elected to drill a third well at the GC 955 site. The selected location is very near the structural crest of the closure, and marks the highest stratigraphic and structural position with strong leading-peak seismic anomalies at this site. Expected depth to base of the stability zone was not well constrained in this location, however, the site was thought to have the potential for thick and possibly multiple gas-hydrate-bearing zones. As at the GC 955-H well, this leading peak is accompanied by strong trough reflections as well, and given the structural location, was assessed as an even greater gas flow risk in the pre-drill hazard analyses (Figures F2, F4, and F11). In addition, the section shows numerous strong amplitudes, both peaks and troughs, below the primary target horizon. However, the findings at the H-well, as well as the Q-4000's ability to pump heavy muds, lead to a decision among the project team to drill the location.

From the seafloor to a depth of about 1320 fbsf, gamma-ray values were variable but generally low, indicating a mud-rich section with minor thin silts and sands. Resistivity throughout this interval steadily increased from $\sim 1 \Omega\text{-m}$ in the shallow section to $\sim 2 \Omega\text{-m}$ near the base of this unit. Despite the well crossing a major fault zone, and the general proximity to the thick fractured-filling hydrate occurrence in the H well to east, the Q well shows little evidence of gas hydrate in the upper mud-rich sediments.

From ~ 1320 fbsf to ~ 1440 fbsf (the deepest obtained gamma-ray reading), gamma-ray values steadily decreased with depth, suggesting the top of a fining-upward sand section. The interval from ~ 1360 to ~ 1410 fbsf consists of thinly-bedded sands with significant clay content that exhibit resistivity of $\sim 1.5 \Omega\text{-m}$ suggesting modest, if any, gas hydrate fill. A tight interval (as noted on the density log 10 feet in thickness occurs from 1410 to 1420 fbsf,

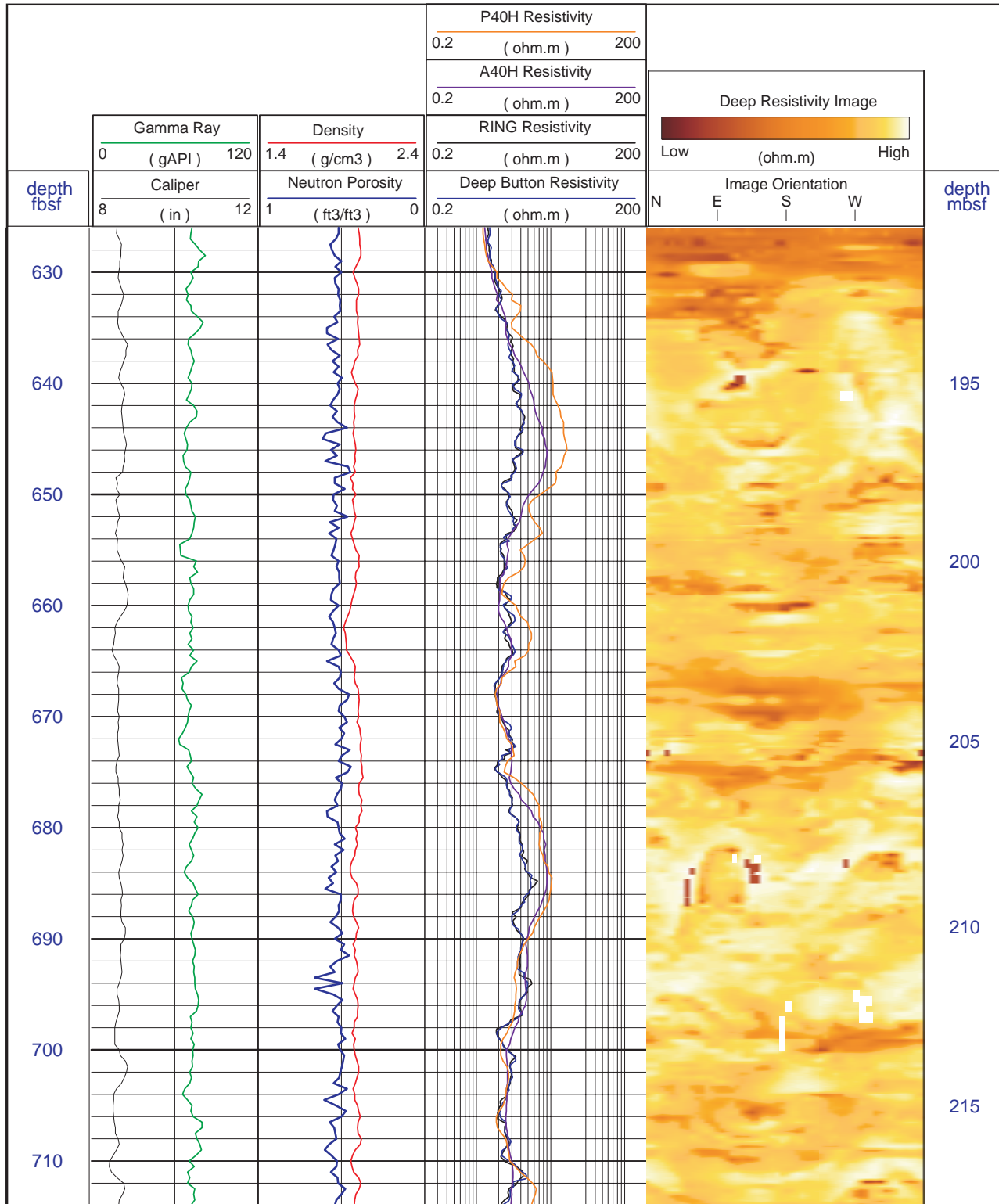


Figure F19: Azimuthal resistivity images inclined fractures grain displacing gas hydrate occurrence at Well GC 955-H (Guerin et al., 2009).

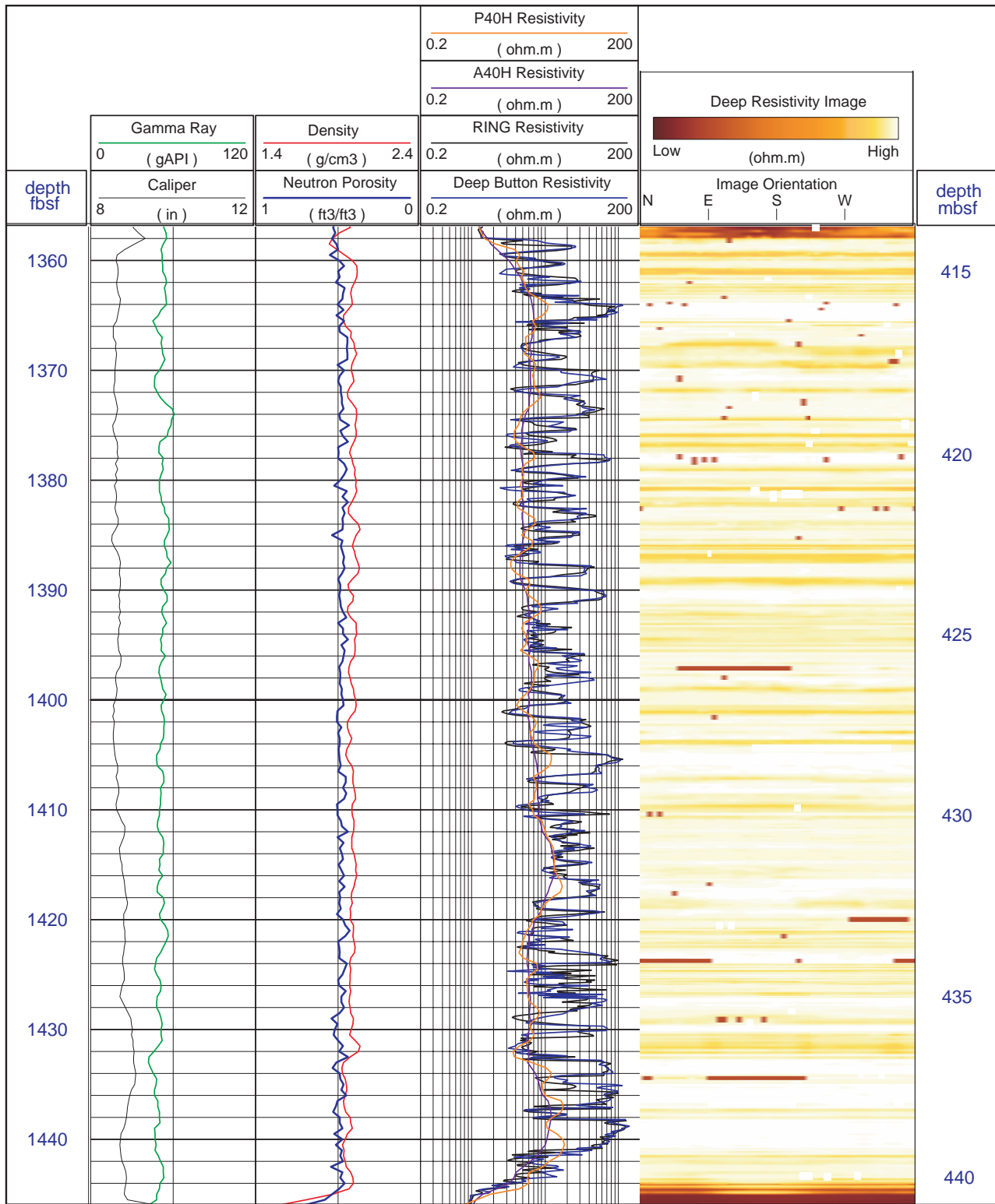


Figure F20: Azimuthal resistivity images from primary gas hydrate target at Well GC 955-H (Guerin et al., 2009).

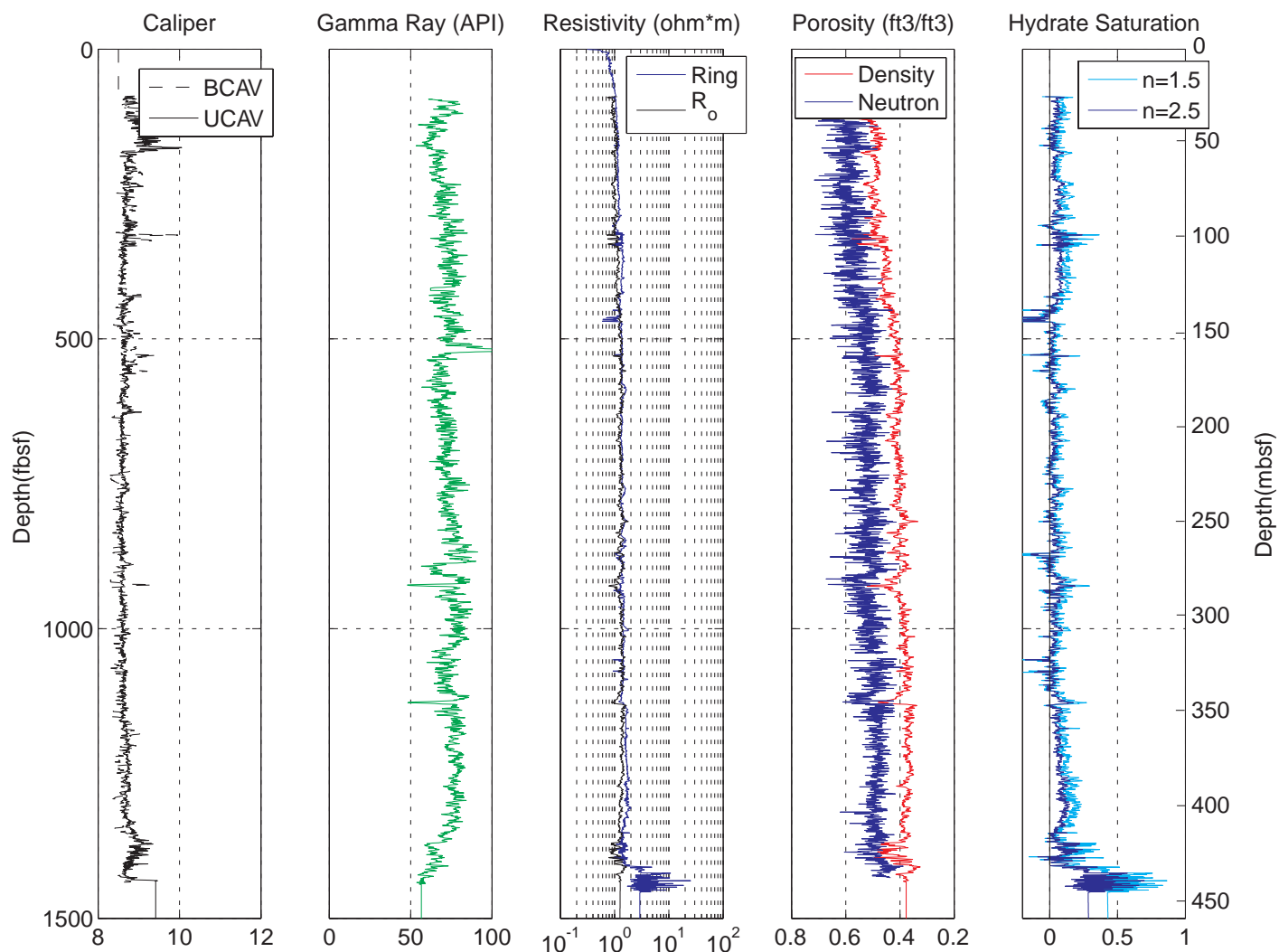


Figure F21: Caliper, gamma, resistivity, density, and hydrate saturation logs at Well GC 955-Q (Guerin *et al.*, 2009).

and below this, porosities and resistivities (up to $10 \Omega\text{-m}$) abruptly increase. From 1420 fbsf to the deepest resistivity reading at 1454 fbsf, resistivities are highly-variable (from 3 to $10 \Omega\text{-m}$, with a few thin spikes to $20 \Omega\text{-m}$) indicating thinly-laminated sand intervals similar to those observed at the H location. The lowest tool on the tool string, the MP3 acoustic tool, shows clearly elevated velocities in the sand section in direct correspondence to the profile of the resistivity curve (Figures F21 and F22), indicating the presence of gas hydrate, but below this, the tool shows a complex velocity structure that may indicate that free gas was penetrated below the gas hydrate. Elevated velocities (greater than 2150 m/s) are recorded to a depth of 1466 fbsf, the deepest LWD reading acquired in the hole, approximately 35 feet above the drill bit.

While drilling at 1498, the ROV recorded a large expulsion of gas and sediment from the borehole. Although this

event was very short-lived, the team immediately began to implement the program's gas flow control protocols, which included cementing and abandoning the well (Collett *et al.*, 2009). At this time, it is not well understood what role gas hydrate, free gas, and potential well-bore disturbances may have played in the gas release and flow issues at the GC 955-Q well. Further log studies, such as shear velocities, may help determine if free gas was penetrated at the bottom of the hole.

Summary

Drilling at GC 955 was designed to test a range of geologic models for the occurrence and geophysical expression of gas hydrate in sand reservoirs. The initial well drilled (GC 955-I) tested a muted seismic anomaly well above the base of gas hydrate stability that appeared to correspond to the stratigraphic level of a potential 20 ft-thick gas hydrate occurrence in a nearby, pre-existing well. By

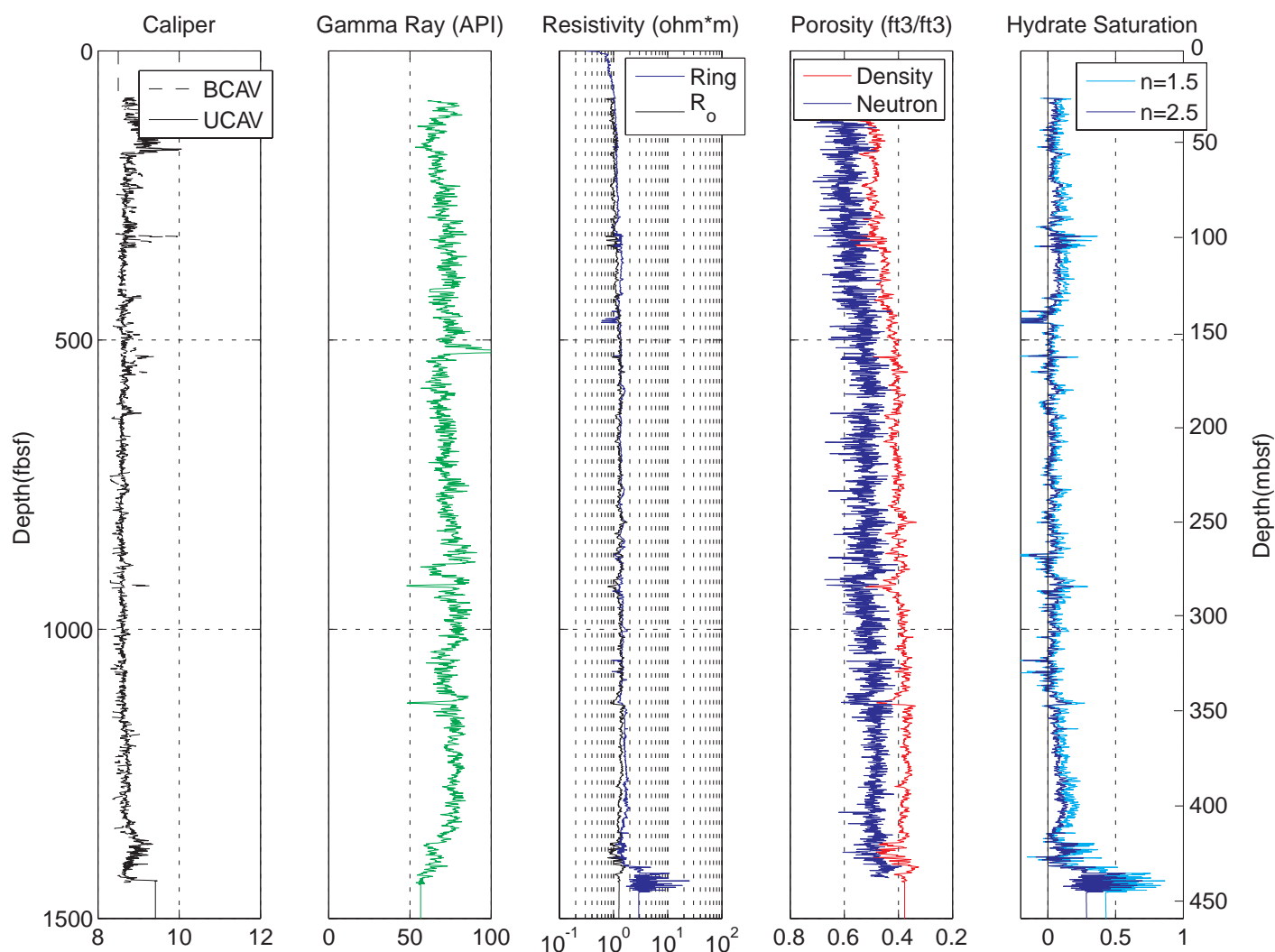


Figure F22: Gamma, resistivity, and sonic logs at Well GC 955-Q (Guerin et al., 2009).

being close to the axis of the major sand dispersal fairway in the region, and being away from the strong indicators of focused flow and gas charging on the closed structure in the southwestern corner of the block, the I-location maximized the opportunity to encounter sand in the GHSZ while minimizing potential drilling hazards. The well did encounter thick, high-quality sands, but these sands were fully water-saturated. Only minor indications of gas hydrate were seen. The second well (GC 955-H) tested compelling direct geophysical indicators for gas hydrate (high-amplitude reflection packages of appropriate polarity) on the flanks of the closed structure and removed from the channel axis. Therefore, the site offered highly prospective targets with only slightly elevated geologic risk (potential lack of reservoir), but significantly greater risk of drilling hazards. The well encountered ~100 feet of highly-saturated gas hydrate in sand reservoirs, in close agreement with pre-drill predictions, and with no indications of free gas.

Unexpectedly, the location also featured a thick fracture-filling gas hydrate occurrence in the overlying muds. In detail, the gas hydrate occurrence at GC 955-H poses many intriguing science questions related to the nature and existence of multiple apparent gas hydrate and water contacts within a single sand unit. The third well (GC 955-Q) tested geophysical targets at the crest of the structure, maximizing the potential for gas hydrate fill. Geologic risk at the well was again elevated, as the location is the most distal from the sand fairway, and drilling risk, while still significant, had been mitigated by the findings at the H well. The well encountered sand as expected, again saturated with gas hydrate. However, only the top of the apparently fining-upwards sand unit was logged, and the true nature and extent of the gas hydrate occurrence is not known. Gas flow issues at the well, presently of unclear origin, resulted in drilling being halted before the zone could be more fully drilled and logged.

The drilling program at GC 955 confirms the integrated geological-geophysical approach used within the JIP program to assess gas hydrate occurrence from remote sensing data. The presence of fluid flow, a petroleum system, and potential reservoir, were primary elements in the exploration model adopted by the JIP for prospecting for gas hydrate accumulations in sands along the gas hydrate stability boundary. Several secondary hypothesis related to the potential occurrence of poorly-imaged gas hydrate were tested; however, no gas hydrate was found in sand reservoirs that was not anticipated by the geophysical analysis. The GC 955 site should provide a wealth of opportunities to advance our understanding of gas hydrate systems, both the continuing evaluation of the LWD data collected in Leg II, and in future additional data collection programs. The multi-component acoustic and high resolution electric logs, used here to assess the gas hydrate targets, will also provide an extraordinary resource for Pleistocene stratigraphic and acoustic studies in the Gulf of Mexico.

References

- Amery, G. B., 1969. Structure of Sigsbee Scarp, Gulf of Mexico, AAPG Bulletin, V. 58, No. 12 (December 1969), P. 2480-2482.
- Anadarko, 2006. Press release, Anadarko strikes 250 ft payzone in US Gulf: Mission Deep, http://www.oilandgasinternational.com/departments/exploration_discoveries/dec06_anadarko.aspx
- Boswell, R., Collett, T.S., Frye, M., McConnell, D., Shedd, W., Mrozewski, S., Guerin, G., and Cook, A., 2009. Gulf of Mexico Gas Hydrate Joint Industry Project Leg II — Technical Summary: Proceedings of the Drilling and Scientific Results of the 2009 Gulf of Mexico Gas Hydrate Joint Industry Project Leg II. <http://www.netl.doe.gov/technologies/oil-gas/publications/Hydrates/2009Reports/TechSum.pdf>
- Collett, T.S., Boswell, R., Mrozewski, S., Guerin, G., Cook, A., Frye, M., Shedd, W., and McConnell, D., 2009. Gulf of Mexico Gas Hydrate Joint Industry Project Leg II — Operational Summary: Proceedings of the Drilling and Scientific Results of the 2009 Gulf of Mexico Gas Hydrate Joint Industry Project Leg II. <http://www.netl.doe.gov/technologies/oil-gas/publications/Hydrates/2009Reports/OpSum.pdf>
- Dai, J., Snyder, F., Gillespie, D., Koesoemadinata, A., Dutta, N., 2008. Exploration for gas hydrates in the deepwater, northern Gulf of Mexico: Part I. A seismic approach based on geologic model, inversion, and rock physics principles. *Journal Marine and Petroleum Geology*, (25), pp. 830-844.
- Frye, M., compiler, 2008. Preliminary Evaluation of in-place Gas Hydrate Resources: Gulf of Mexico Outer Continental Shelf: MMS OCS Report 2008-004. <http://www.mms.gov/revaldiv/GasHydrateFiles/MMS2008-004.pdf>
- Guerin, G., Cook, A., Mrozewski, S., Collett, T.S., Boswell, R., 2009. Gulf of Mexico Gas Hydrate Joint Industry Project Leg II — Green Canyon 955 LWD Operations and Results: Proceedings of the Drilling and Scientific Results of the 2009 Gulf of Mexico Gas Hydrate Joint Industry Project Leg II. <http://www.netl.doe.gov/technologies/oil-gas/publications/Hydrates/2009Reports/GC955LWDops.pdf>
- Heggland, R., 2004. Definition of geohazards in exploration 3-D seismic data using attributes and neural-network analysis, AAPG Bull. V. 88, No. 6 (June 2004), p. 857-868
- Hutchinson, D.R., Shelander, D., Dai, J., McConnell, D., Shedd, W., Frye, M., Ruppel, C., Boswell, R., Jones, E., Collett, T., Rose, K., Dugan, B., Wood, W., and Latham, T., 2008. Site Selection for DOE/JIP Gas Hydrate Drilling in the Northern Gulf of Mexico: Sixth International Conference on Gas Hydrates, Vancouver, BC., 7-10 July, 2008. <https://circle.ubc.ca/handle/2429/1165>.
- Hutchinson, D., Boswell, R., Collett, T.S., Dai, J., Dugan, B., Frye, M., Jones, E., McConnell, D., Rose, K., Ruppel, C., Shedd, W., Shelander, D., Wood, W., 2009. Gulf of Mexico Gas Hydrate Joint Industry Project Leg II — Green Canyon 955 Site Selection: Proceedings of the Drilling and Scientific Results of the 2009 Gulf of Mexico Gas Hydrate Joint Industry Project Leg II. <http://www.netl.doe.gov/technologies/oil-gas/publications/Hydrates/2009Reports/GC955SiteSelect.pdf>

- McConnell, D. R., 2000. Optimizing deepwater well locations to reduce the risk of shallow-water-flow using high resolution 2-D and 3-D seismic data: Proceedings, Offshore Technology Conference, Houston, Texas 1 4 May 2000, OTC 11973.
- McConnell, D., and Zhang, Z., 2005. Using acoustic inversion to image buried gas hydrate distribution: FITI newsletter, Fall, 2005, p. 3-5, http://www.netl.doe.gov/technologies/oil-gas/publications/Hydrates/Newsletter/HMNewsFall05_HighRez.pdf#page=3
- Mrozewski, S., Guerin, G., Cook, A., Collett, T.S., Boswell, R., 2009. Gulf of Mexico Gas Hydrate Joint Industry Project Leg II — LWD Methods: Proceedings of the Drilling and Scientific Results of the 2009 Gulf of Mexico Gas Hydrate Joint Industry Project Leg II. <http://www.netl.doe.gov/technologies/oil-gas/publications/Hydrates/2009Reports/LWDMethods.pdf>
- Nagihara, S. and M. A. Smith, 2008. Regional overview of deep sedimentary thermal gradients of the geopressured zone of the Texas-Louisiana continental shelf, AAPG Bulletin, V. 92, No. 1 (January 2008), P. 1-14
- Nibbelink, K., 1999. Modeling deepwater reservoir analogs through analysis of recent sediments using coherence seismic amplitude, and bathymetry data, Sigsbee Escarpment, Green Canyon, Gulf of Mexico, The Leading Edge, May, 1999, p. 550
- Nur, A. and J. Dvorkin, 2008. Seismic-scale rock physics of methane hydrate – Final report, prepared by Stanford University for the National Energy Technology Laboratory.
- Orange, D. L. and N. A. Breen, 1992. The effects of fluid escape on accretionary wedges – seepage force, slope failure, headless submarine canyons, and vents, Journal of Geophysical Research, vol, 97. no. B6, p. 9277-9295
- Orange, D. L., D. Saffer, P. Jeanjean, Z. Al-Khafaji, G. Riley and G. Humphrey, 2003. Measurements and modeling of the shallow pore pressure regime at the Sigsbee Escarpment: successful prediction of overpressure and ground-truthing with borehole measurements, Proceedings, Offshore Technology Conference, Houston, Texas 5 8 May 2003, OTC 15201
- Rowan, M. G., M. P. A. Jackson, and B. D. Trudgill, 1999. Salt-Related fault families and fault welds in the northern Gulf of Mexico, AAPG Bulletin, V. 83, No. 9 (September 1999), P. 1454-1484
- Shedd, W., Godfriaux, P., Frye, M., Boswell, R., and Hutchinson, D., 2009. Occurrence and variety in seismic expression of the base of gas hydrate stability in the Gulf of Mexico, USA: FITI newsletter, Winter, 2009, p. 11-14, <http://www.netl.doe.gov/technologies/oil-gas/publications/Hydrates/Newsletter/MHNewswinter09.pdf>
- Swiercz, A. M., 1991. Seismic stratigraphy and salt tectonics along the Sigsbee Escarpment, southeastern Green Canyon region, in Geyer, R. A. and M. Ashwell eds., CRC handbook of geophysical exploration at sea: hydrocarbons: CRC Press, Boca Raton, FL., 496 p.
- Weimer, P., 1990. Sequence stratigraphy, facies geometries, and depositional history of the Mississippi Fan, Gulf of Mexico, AAPG Bull. V. 74. No. 4, p. 425-453